AN ADAPTIVE ARRAY FOR INTERFERENCE REJECTION

R.L. Riegler and R.T. Compton, Jr.

The Ohio State University
ElectroScience Laboratory
Department of Electrical Engineering
Columbus, Ohio 43212

REPORT 2552-4

16 February 1970

Grant Number NGR 17-004-013

National Aeronautics and Space Administration
Office of Grants and Research Contracts
Washington, D.C. 20546
and
University of Kansas
Center for Research
CRES 1091-1

NOTICES

When Government drawings, specifications, or other data are used for any purpose other than in connection with a definitely related Government procurement operation, the United States Government thereby incurs no responsibility nor any obligation whatsoever, and the fact that the Government may have formulated, furnished, or in any way supplied the said drawings, specifications, or other data, is not to be regarded by implication or otherwise as in any manner licensing the holder or any other person or corporation, or conveying any rights or permission to manufacture, use, or sell any patented invention that may in any way be related thereto.

AN ADAPTIVE ARRAY FOR INTERFERENCE REJECTION

R.L. Riegler and R.T. Compton, Jr.

REPORT 2552-4

16 February 1970

Grant Number NGR 17-004-013

National Aeronautics and Space Administration
Office of Grants and Research Contracts
Washington, D.C. 20546
and
University of Kansas
Center for Research
CRES 1091-1

ABSTRACT

An adaptive array that rejects undesired or interfering signals is presented. The array pattern is controlled by an adaptive feedback system based on a steepest-descent minimization of mean square error. Here error is defined as the difference between the array output and a locally generated reference signal. Minimization of mean square error is closely related to maximization of signal-to-noise ratio.

A 2-element adaptive array has been built, and its experimental performance is discussed. Typical patterns for various desired and interfering signals are shown, as well as measured transient response. Finally, some experiments showing the array behavior with modulated signals are described.

The results show that such an antenna system is capable of automatically rejecting interfering signals, subject only to certain basic constraints. No a priori information concerning the angles of arrival of the signals is required. Detailed knowledge of the waveforms of the desired and interfering signals is also not needed, although the spectral density of the desired signal must be known.

CONTENTS

AN ADAPTIVE ARRAY FOR INTERFERENCE REJECTION

I. INTRODUCTION

An adaptive array may be defined as one that modifies its own pattern, frequency response, or other parameters, by means of internal feedback control, while the antenna operates. All adaptive antennas to date have been receiving arrays, because the pattern of a receiving array can be easily controlled by individually adjusting the amplitude and phase of the signal from each element. However, other types of adaptive antenna configurations are conceivable.

A phase-lock loop array[1] is probably the best known type of adaptive array. A phase-lock loop array operates by aligning the phase of the signal from each element with that of a reference signal*, with a phase-lock loop, before the signals are summed. This type of feedback forces the antenna to have a beam in the direction of the incoming signal. Amplitude control of the signal from each element is sometimes added, giving additional flexibility to the pattern control. Svoboda[1] discusses an amplitude control scheme that sets the gain of each element proportional to the ratio of rms signal level to noise power on that element, thus making the array operate as a maximal-ratio combiner[2]. The self-phasing array has certain desirable features (automatic beam tracking and an adaptive bandwidth), but it also has undesired features, the most important being the susceptibility of the array to being "captured" by interference or jamming[3].

An entirely different type of adaptive array has recently been proposed by Shor[4], and also by Widrow, et al.[5]. Their approach has been more general - namely, to look on the adjustment of the weighting coefficients in the array as an adaptive optimization problem. Shor adjusts the weights in the array to maximize the signal-to-noise ratio at the output. Widrow, et al., minimize an error signal, which is equal to the difference between the output of the array and a reference signal. It can be shown that these two criteria are closely related.

In this report we discuss an experimental adaptive array based on the feedback concept discussed by Widrow, et al.[5]. The general form of the adaptive array is shown in Fig. 1. The signal from each element is passed through an amplifier with controllable gain and phase. The signals are then added to produce the array output S(t). To make the array adaptive, S(t) is compared with a reference signal T(t), and the difference, the error signal $\varepsilon(t)$, forms the input to a feedback system

---

*The reference signal can be (1) the signal on one of the elements, (2) the sum signal from the array, or (3) a locally generated reference signal.

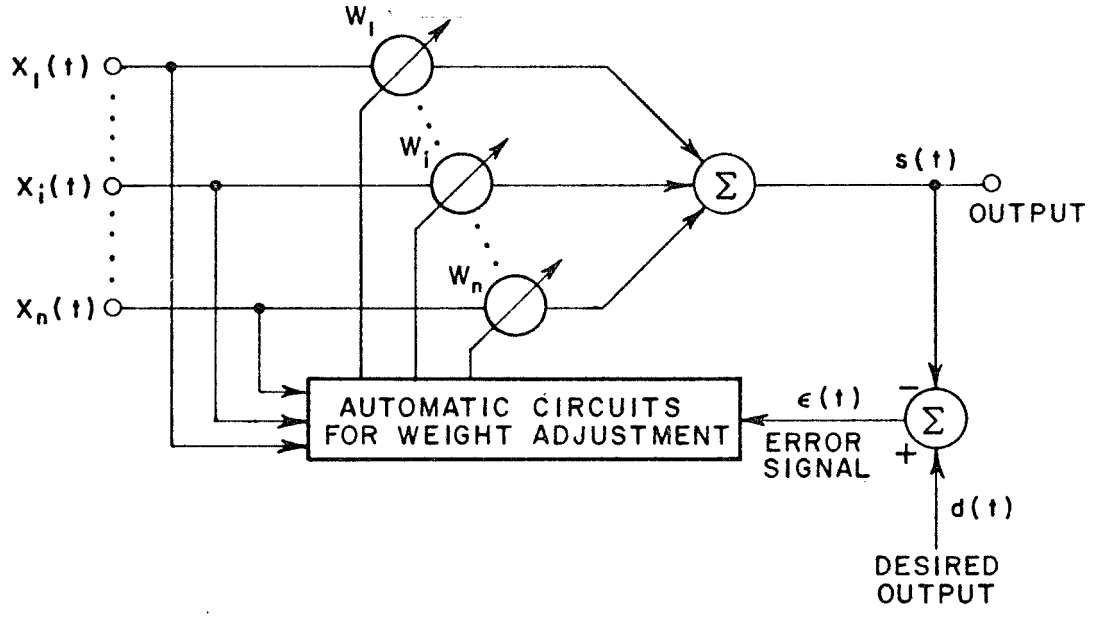

Fig. 1. Basic adaptive feedback system.

that controls the weights w_i. The feedback is designed to adjust the weights so the mean-square value of $\varepsilon(t)$ is minimized. This has the effect of forcing the output of the array $S(t)$ to approximate the reference signal $T(t)$ as closely as possible on a mean-square basis. Thus, any received signal that is not represented in $T(t)$ appears as an error signal, and the feedback adjusts the weights to remove it from the output. The result, in antenna parlance, is a pattern null in the direction from which this signal comes. If the received signal is represented in $T(t)$, the feedback retains this signal in the output (with amplitude and phase the same as $T(t)$). Thus, one can discriminate between "desired" and "undesired" signals (e.g., between a desired communication signal and an interfering signal) by means of what is used for the reference signal $T(t)$.

The feedback concept discussed above was suggested by Widrow, et al.[5]. The work described here differs from their work, however, in several respects. First, we are interested mainly in the problem of interference rejection in radio communications. To treat this problem realistically, it must be assumed that the desired signal contains modulation components that are unknown at the receiver.

Hence the reference signal T(t) cannot be made exactly equal to the desired signal, but can only approximate it in some sense. We describe here some experiments in which the desired signal contains modulation components not present on the reference signal. Widrow, et al. treat the case where the desired signal is known exactly at the receiver, so an exact replica can be used for the reference T(t). Second, the feedback system discussed here is a continuous, analog system. Widrow, et al., consider a digital, sampled-data feedback loop. Although this is only a minor difference, the problems of feedback loop stability, which are discussed in some detail in [5], arise only with a sampled loop. A continuous loop, based on the feedback algorithm discussed below, is stable for all gain settings. Third, the work reported here is primarily experimental, whereas the work in [5] is theoretical.

II. THE FEEDBACK ALGORITHM

Let us assume for the moment that the weighting coefficients $w_1, \ldots, w_N$ shown in Fig. 1 are real. That is, we ignore the possibility of varying the phase of each element. The array output may then be written

$$(1) \qquad s(t) = \sum_{i=1}^{N} w_i x_i(t).$$

The error signal is

$$(2) \qquad \varepsilon(t) = T(t) - \sum_{i=1}^{N} w_i x_i(t),$$

and hence the squared error is

$$(3) \qquad \varepsilon^2(t) = T^2(t) - 2T(t) \sum_{i=1}^{N} w_i x_i(t) + \sum_{i=1}^{N} \sum_{j=1}^{N} w_i w_j x_i(t) x_j(t).$$

The mean-square error is thus:

$$(4) \qquad \overline{\varepsilon^2(t)} = \overline{T^2(t)} - 2 \sum_{i=1}^{N} w_i \, \overline{T(t) x_i(t)} + \sum_{i=1}^{N} \sum_{j=1}^{N} w_i w_j \, \overline{x_i(t) x_j(t)}$$

where the bar indicates the time average. Equation (4) may be written more conveniently in matrix form as

$$(5) \qquad \overline{\varepsilon^2(t)} = \overline{T^2(t)} - 2W^T \Phi(x,T) + W^T \Phi(x,x) W$$

where w and $\Phi(x,T)$ are column matrices,

$$(6) \qquad w = \begin{pmatrix} w_1 \\ w_2 \\ \cdot \\ \cdot \\ \cdot \\ w_N \end{pmatrix},$$

$$(7) \qquad \phi(x,T) = \begin{pmatrix} \overline{x_1(t)\ T(t)} \\ \overline{x_2(t)\ T(t)} \\ \cdot \\ \cdot \\ \cdot \\ \overline{x_N(t)\ T(t)} \end{pmatrix},$$

$\Phi(x,x)$ is an N x N matrix,

$$(8) \qquad \Phi(x,x) = \begin{pmatrix} \overline{x_1(t)\ x_1(t)} & \overline{x_1(t)\ x_2(t)} & \cdots & \overline{x_1(t)\ x_N(t)} \\ \overline{x_2(t)\ x_1(t)} & & & \cdot \\ \cdot & & & \cdot \\ \cdot & & & \cdot \\ \cdot & & & \cdot \\ \overline{x_N(t)\ x_1(t)} & \cdots & & \overline{x_N(t)\ x_N(t)} \end{pmatrix}$$

and w^T denotes the transpose of w.

It may be seen from Eq. (4) or (5) that $\overline{\varepsilon^2(t)}$ is a quadratic function of the weights. Thus, if it is assumed that $\overline{x_i(t)\ x_j(t)}$ and $\overline{x_i(t)\ T(t)}$ are constant, the surface obtained by plotting $\overline{\varepsilon^2(t)}$ versus the weights is a bowl-shaped surface, as illustrated in Fig. 2 for the case of two weights. (The case where $\overline{x_i(t)\ x_j(t)}$ and $\overline{x_i(t)\ T(t)}$ change with time* may be viewed as a motion of the bowl.) The quadratic nature

---

*These time averages are understood to be taken over an interval long compared with the fluctuations of $x_i(t)$ and T(t), but still finite, so gradual changes in the characteristics of the signals result in time-changing averages.

of Eq. (4) is important, because it implies that the bowl has a well-defined minimum, and furthermore it has only one minimum. Thus, saddle-points or relative minima are not possible.

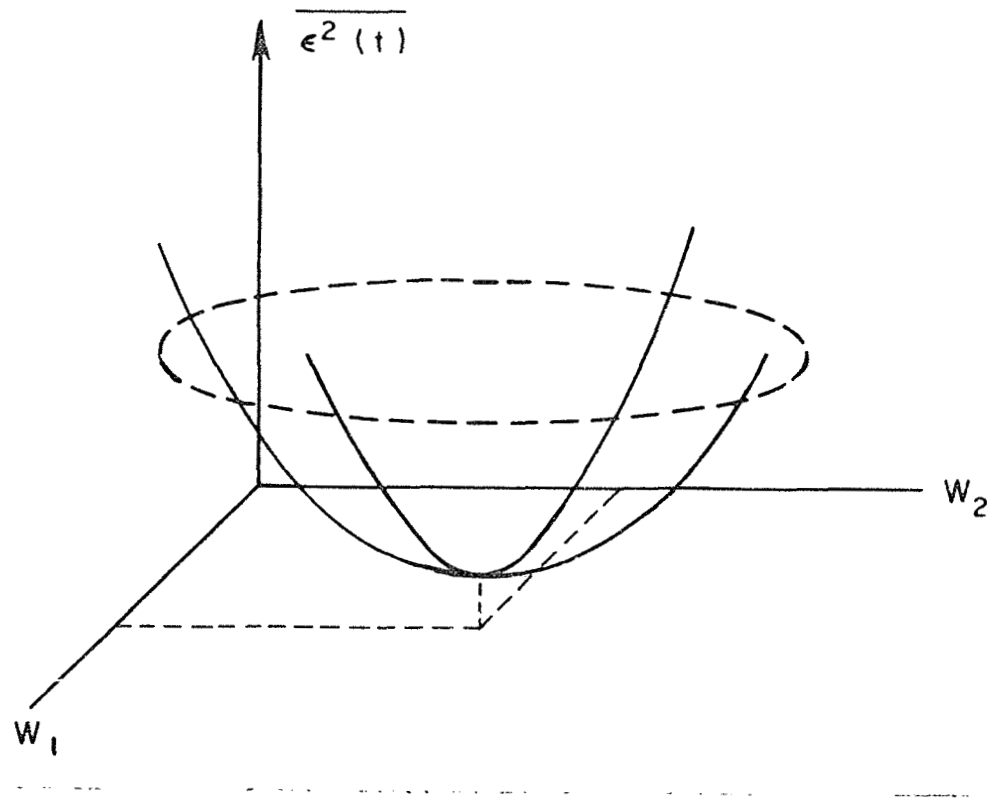

Fig. 2. The error surface.

It is clear on physical grounds that the extremum of the bowl is a minimum, not a maximum, since the error can be made arbitrarily large by a suitable setting of the weights. The value of the weight vector giving minimum $\overline{\varepsilon^2(t)}$, which we will denote by $w_{opt.}$, may be found by setting

$$\nabla_w(\overline{\varepsilon^2}) = 0, \tag{9}$$

where ∇_w denotes the gradient with respect to w. Since

$$\nabla_w(\overline{\varepsilon^2}) = -2\Phi(x,T) + 2\Phi\,(x,x)\,w, \tag{10}$$

we find

(11) $$\Phi(x,x)w_{opt.} = \Phi(x,T)$$

or

(12) $$w_{opt.} = \Phi(x,x)^{-1}\,\Phi(x,T),$$

where we have assumed that $\Phi(x,x)$ is nonsingular so its inverse $\Phi(x,x)^{-1}$ exists. If the weight vector w is set equal to $w_{opt.}$, the resulting minimum mean-square error is found from Eq. (5) to be

(13) $$\overline{\varepsilon^2_{min}} = \overline{T^2(t)} - \Phi^T(x,T)\,\Phi^{-1}(x,x)\,\Phi(x,T).$$

This result may be used to rewrite Eq. (5) in the form

(14) $$\overline{\varepsilon^2(t)} = \overline{\varepsilon^2_{min}} + (w-w_{opt.})^T\,\Phi(x,x)\,(w-w_{opt.}),$$

which places the quadratic dependence of $\overline{\varepsilon^2(t)}$ on the weights w_i clearly in evidence. Finally, we remark that the "bowl" does not necessarily have its principle axes oriented parallel to the w_i-axes. A coordinate system whose axes do lie parallel to the principle axes may be defined by the relation:

(15) $$w-w_{opt.} = R\ell$$

where R is an N x N rotation matrix of elements r_{ij}:

(16) $$R = \begin{pmatrix} r_{11} & r_{12} & \cdots & r_{1N} \\ \vdots & & & \\ r_{N1} & & \cdots & r_{NN} \end{pmatrix}$$

and ℓ is an N-element column matrix whose elements ℓ_i are the "normal coordinates" of the bowl:

(17) $$\ell = \begin{pmatrix} \ell_1 \\ \vdots \\ \ell_N \end{pmatrix}$$

Substituting Eq. (15) into Eq. (14) gives

$$\overline{\varepsilon^2(t)} = \overline{\varepsilon^2_{min}} + \ell^T [R^T \Phi(x,x) R] \ell \tag{18}$$

and when R is chosen so $R^T \Phi(x,x)R$ is diagonal,

$$R^T \Phi(x,x) R = \Lambda = \begin{pmatrix} \lambda_1 & 0 & 0 & \cdots \\ 0 & \lambda_2 & 0 & \cdots \\ 0 & 0 & \cdot & \\ \cdot & \cdot & \cdot & \\ \cdot & \cdot & \cdot & \\ \cdot & \cdot & & \lambda_N \end{pmatrix} \tag{19}$$

then the ℓ_i are normal coordinates. We note that since the $\overline{\varepsilon^2(t)}$ surface has a minimum for $w = w_{opt.}$, the eigenvalues λ_i are nonnegative. The fact that $\lambda_i \geq 0$ may also be shown directly from $\Phi(x,x)$, but we will not go through that here.

Now let us examine the justification for using minimum mean-square error as the criterion for optimizing array performance. In general, the output from the array consists of three types of contributions: a desired signal, an interfering signal, and random noise. We may write

$$S(t) = \alpha S_d(t) + \beta S_i(t) + \gamma n(t) \tag{20}$$

where

$S_d(t)$ = a desired signal

$S_i(t)$ = an interfering signal

$n(t)$ = random noise

and where α, β, and γ are constants representing the combined effect of the weights w_i on these signals. Assume for the moment that the waveform of the desired signal is known exactly at the receiver. Then if the reference signal $T(t)$ is set equal to a replica of the desired signal,

$$T(t) = S_d(t) \tag{21}$$

the error signal becomes

$$\varepsilon(t) = T(t) - S(t) = (1-\alpha)\, S_d(t) - [\beta S_i(t) + \gamma n(t)] \tag{22}$$

where the terms $S_d(t)$, $S_i(t)$ and $n(t)$ are assumed uncorrelated, so the cross-product terms, such as $\overline{S_d(t)\ S_i(t)}$, are zero. Thus, to minimize $\varepsilon^2(t)$, the sum of $(1-\alpha)^2\ S_d^2(t)$ and $\beta^2\ S_i^2(t) + \gamma^2\ n^2(t)$ must be minimized. In general terms, this quantity will be minimum if α is nearly unity and β^2 and γ^2 are as small as possible. But this condition is equivalent to (1) miniziming the power in the interference while (2) constraining the power in the desired signal to be constant. Stated another way, minimizing $\overline{\varepsilon^2}$ is equivalent to maximizing the signal-to-noise ratio, where "noise" is interpreted as including the interference.

This argument, although generally correct, does overlook certain limitations. First, in practice one cannot set $T(t) = S_d(t)$ because the exact form of the desired signal is unknown at the receiver. However, in many cases $T(t)$ can be made to approximate $S_d(t)$ in some sense. For example, when $S_d(t)$ is a signal with amplitude modulation, it is possible to use the carrier component of $S_d(t)$ for $T(t)$ and still obtain suitable operation (as will be seen in the experiments described below). The presence of the sideband components in $S_d(t)$ increases the minimum mean-square error $\overline{\varepsilon^2}_{min}$, but minimizing $\overline{\varepsilon^2}$ still corresponds to maximizing signal-to-noise ratio.

A second limitation is that the arguments break down for low signal-to-noise ratios in the elements. At low SNR's, the array may not tend to constrain $\alpha \approx 1$, if the $S_d(t)$ term contributes only negligibly to $\varepsilon^2(t)$. Thus for low SNR conditions, minimum $\overline{\varepsilon^2}$ may no longer correspond to maximum SNR. However, for most cases, minimizing $\overline{\varepsilon^2}$ is equivalent to maximizing SRN, and this is the optimization criterion used in the array described below.

Now consider the method by which the weights are to be set equal to their optimum values. One approach is to measure the quantities $\overline{x_i(t)\ x_j(t)}$ and $\overline{x_i(t)\ T(t)}$ for all i,j, and thus determine the matrices $\Phi(x,x)$ and $\Phi(x,T)$. $\phi(x,x)^{-1}$ may then be computed, and the optimum weights evaluated by means of Eq. (12). From a practical standpoint, this approach is not appealing, because of the difficulty in measuring $\Phi(x,x)$ and computing $\phi^{-1}(x,x)$, especially if the number of elements is large. Furthermore, the object is to build an adaptive array, so that, for example, changes in the angle of arrival of the interfering signal will be automatically "tracked" by the weight settings. To adapt to such changes by the above method would require that the measurement of $\phi(x,x)$ and $\phi(x,T)$ and the computation of $\phi(x,x)^{-1}$ be repeated periodically.

A more attractive alternative is to use the feedback algorithm suggested in [5]. This feedback rule is based on a steepest descent minimization of ε^2 (not $\overline{\varepsilon^2}$). Specifically, each weight w_i is to be adjusted according to the rule:

$$\frac{dw_i}{dt} = k_s \nabla_{w_i} [\varepsilon^2(t)] \tag{23}$$

where $\nabla_{w_i}[\varepsilon^2(t)]$ denotes the i^{th} component of the gradient of $\varepsilon^2(t)$ with respect to the weight vector w, and k_s is a negative constant. Since the gradient measures the sensitivity of $\varepsilon^2(t)$ to each of the weights, the feedback rule states that a given weight w_i will be changed at a rate proportional to the sensitivity of the $\varepsilon^2(t)$ surface to that weight. The gradient of a surface is a vector in the maximum uphill direction, so $k_s \nabla_N[\varepsilon^2(t)]$ points in the maximum downhill direction. Hence this is a steepest-descent algorithm, and it has also been referred to as the LMS algorithm[5].

Evaluating the gradient gives

$$\nabla_{w_i}[\varepsilon^2(t)] = 2\varepsilon(t)\ \nabla_{w_i}[\varepsilon(t)] \tag{24}$$

and from Eq. (2),

$$\nabla_{w_i}[\varepsilon(t)] = -x_i(t). \tag{25}$$

Hence the feedback rule becomes

$$\frac{dw_i}{dt} = -2k_s x_i(t)\ \varepsilon(t) \tag{26}$$

or in integral form

$$w_i(t) = w_i(0) - 2k_s \int_{t'=0}^{t} x_i(t')\ \varepsilon(t')dt' \tag{27}$$

This feedback may be instrumented as shown in Fig. 3, which shows one loop of the system.

So far we have assumed that the weighting coefficients in the array are real, so that only the amplitudes of the signals $x_i(t)$ are adjusted. Actually, it is necessary to adjust the phase of each signal $x_i(t)$ as well, to make use of the full flexibility available in the pattern. Phase control can be achieved by splitting the signal from each element into an in-phase component and a quadrature component and then adjusting each with

a real weighting coefficient, as shown in Fig. 4. The signal is used directly for the in-phase component, and is delayed one quarter wavelength* to produce the quadrature component. Independent control of the two weights is then equivalent to control of both magnitude and angle.

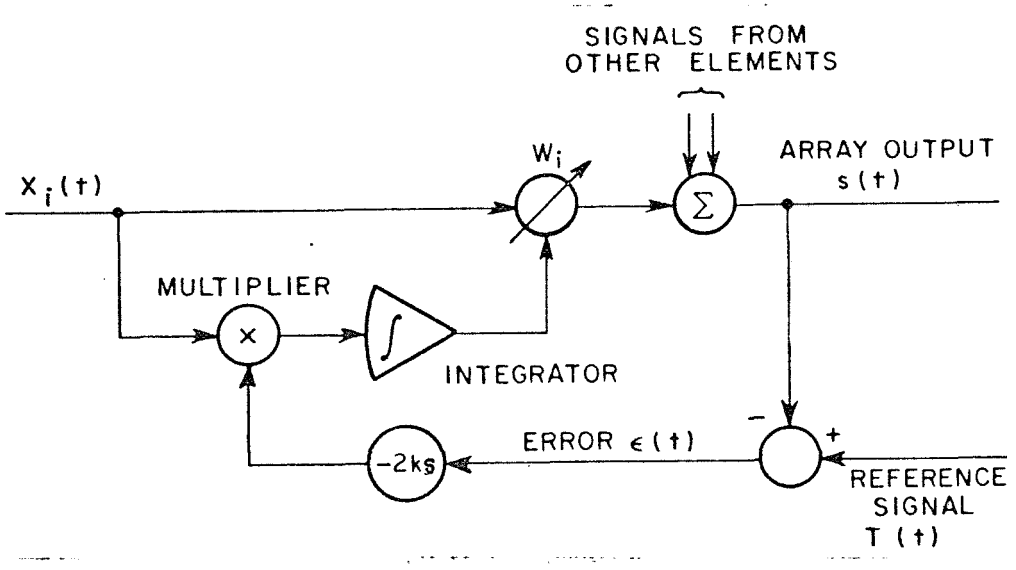

Fig. 3. Basic feedback algorithm.

III. THE PROCESSING UNITS

Two signal processing units based on the feedback scheme shown in Fig. 4 were designed and built. Figure 5 shows a photograph of one of these units. Figure 6 shows the various electronic functions in this unit in more detail. The signal from the element is split into an in-phase channel and a quadrature channel, as discussed above. Each channel is then split again into two parallel paths, one to provide positive gain and the other negative gain. To achieve a full 360° phase control in the unit requires both the in-phase channel and the quadrature channel to be capable of having either positive or negative gain. In practice, this is most easily accomplished by using two amplifiers "back-to-back", one with positive gain and the other with negative gain.

---

*The system described below is relatively narrowband (3 MHz bandwidth at a center frequency of 65 MHz) and the delay required was one-quarter wavelength at 65 MHz.

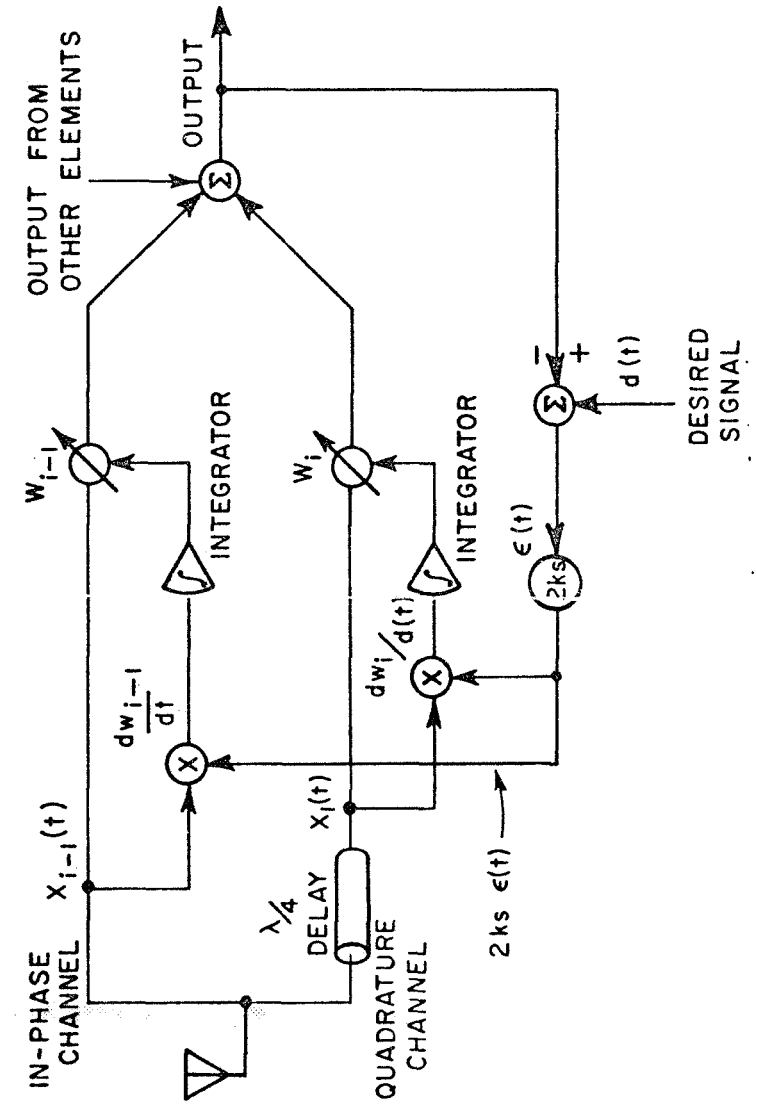

Fig. 4. Feedback Circuit for Each Element

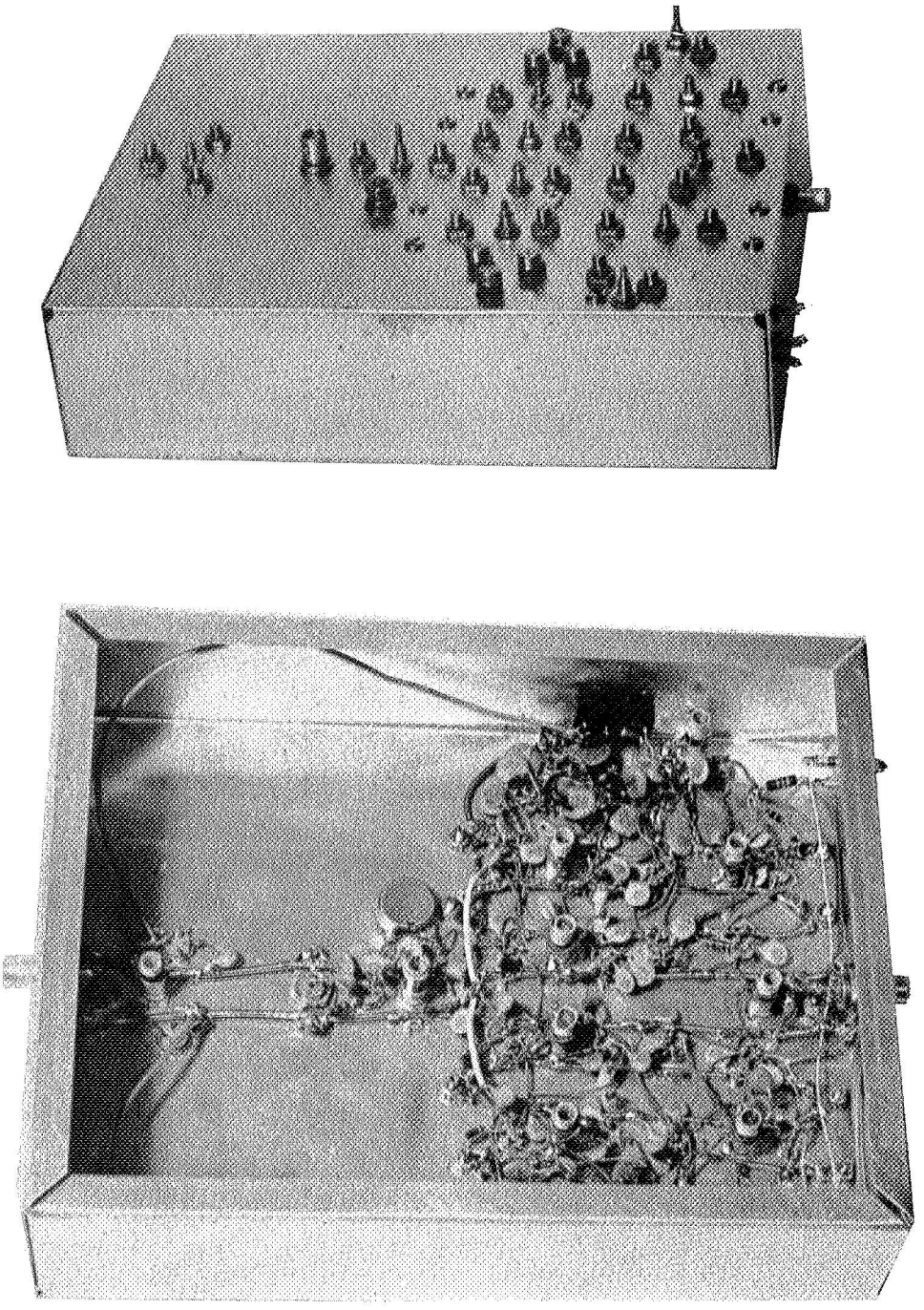

Fig. 5. Electronics Unit for One Element.

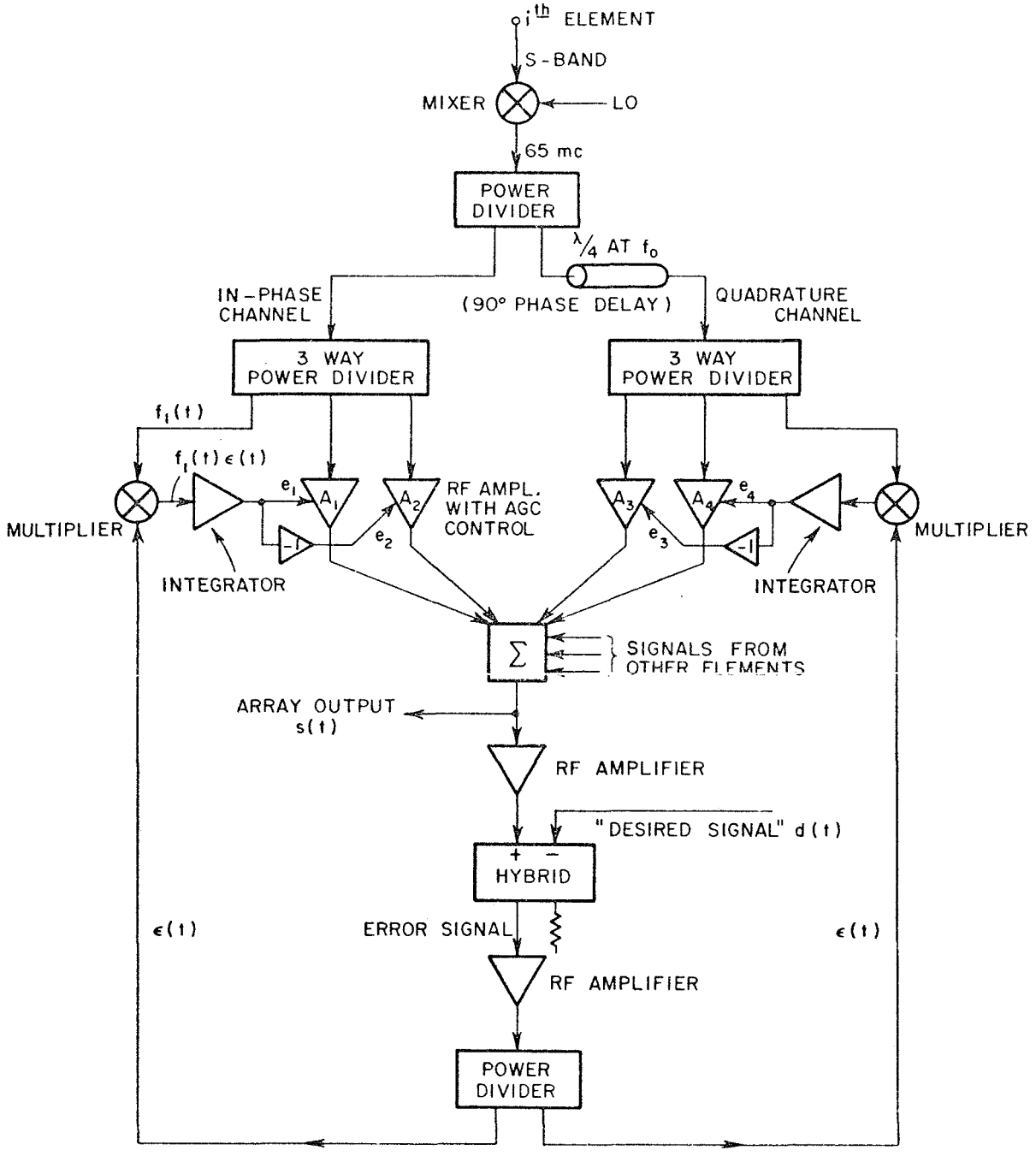

Fig. 6. Adaptive Processing Unit.

The amplifiers used were dual-gate field effect transistors (FET's), which were found to be superior to integrated circuit AGC amplifiers or current controlled diode attenuators with regard to cross-modulation, linearity and phase stability*. In addition, FET amplifiers have the helpful property that the input impedance at the control gate is essentially infinite, so it is possible to "freeze" the weighting coefficients in the array by simply disconnecting the control voltages.

The processing units operate at a center frequency of 65 mHz with an RF bandwidth of approximately 3 mHz. A complete schematic of the processing units is shown in the Appendix.

Figure 7 shows some experimentally measured gain curves for one of the "back-to-back" amplifiers. The plot shows the RF output voltage from the amplifiers as a function of the control voltage, for various input signal levels. Although the curves are not completely linear at lower power levels, the performance was acceptable.

IV. EXPERIMENTAL RESULTS

In this section the results of several experiments performed on a two-element adaptive array, using the processing units described above, are given.

A. Phase Tracking

First, consider the following experiment. An unmodulated signal is fed into both processing units and also into the reference signal port. The adaptive feedback should then adjust both the amplitude and phase of the output signal until they match those of the reference signal (it must minimize the error). Figure 8 shows the measured difference in phase and amplitude between the array output and the reference signal as the phase difference between the two elements is varied over a 360^{o} range. (This is equivalent to varying the angle of arrival of the signal.) It is seen that the phase error varied between -5^{o} and 9^{o} and the amplitude ratio varied over a range of -0.5 dB to +0.4 dB.

B. Amplitude Tracking

Next, Fig. 9 shows the results of an experiment in which the amplitude of the signal was varied, while the reference signal was held constant. The curve shows the amplitude of the error signal $\varepsilon(t)$, relative to the reference signal amplitude. (The lower the error, the

---

*The phase shift of the amplifiers should not change as the gain is adjusted. In practice, it was found that with FET's the phase shift could be held to within 10^{o} over a 25 dB range of gain control.

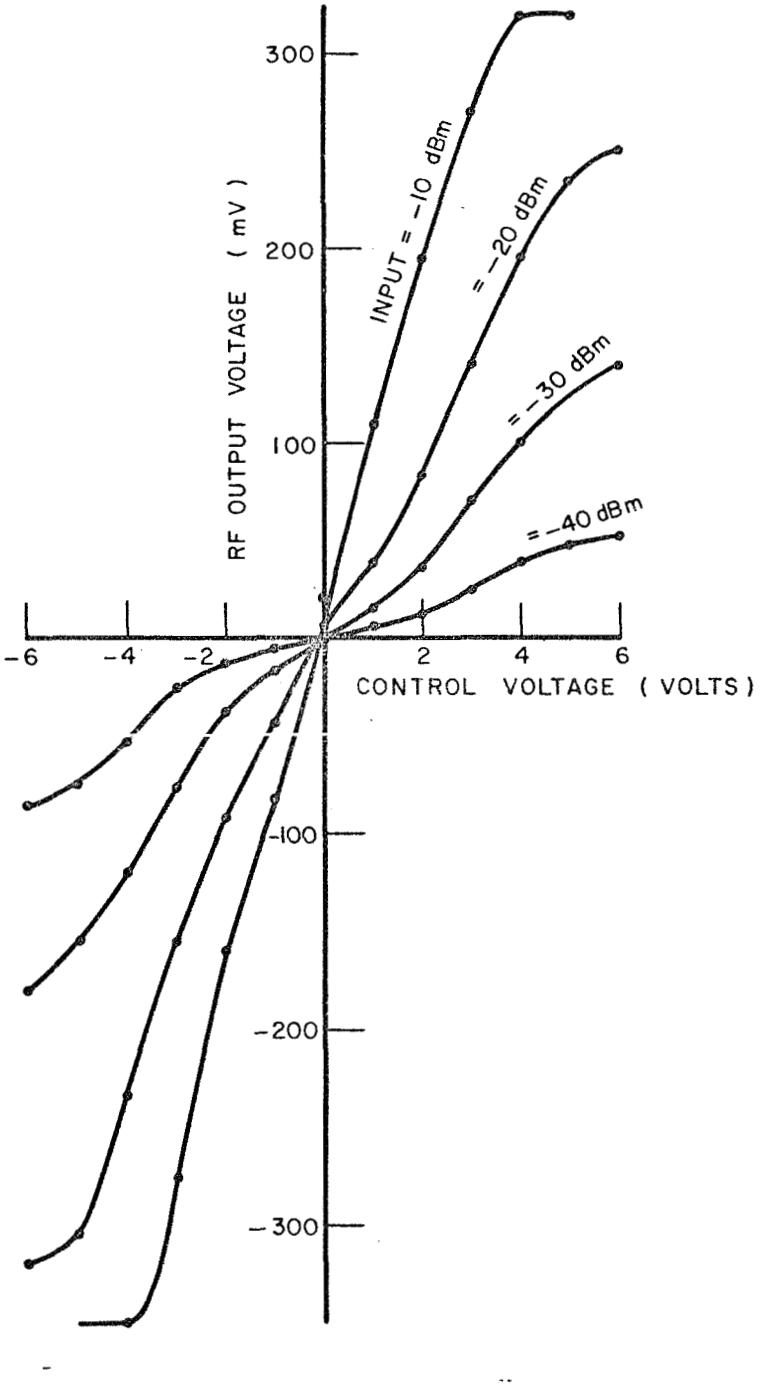

Fig. 7. Amplifier Gain Characteristics.

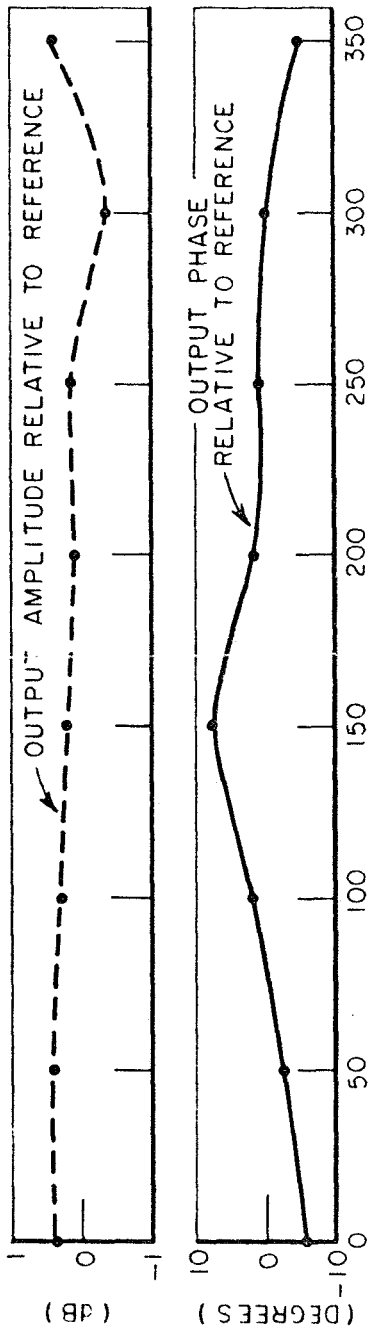

Fig. 8. Input Phase Difference Between Elements.

better the array processing units are performing.) It may be seen that the error was maintained 20 dB or more below the reference over a range of input signal levels of approximately 23 dB.

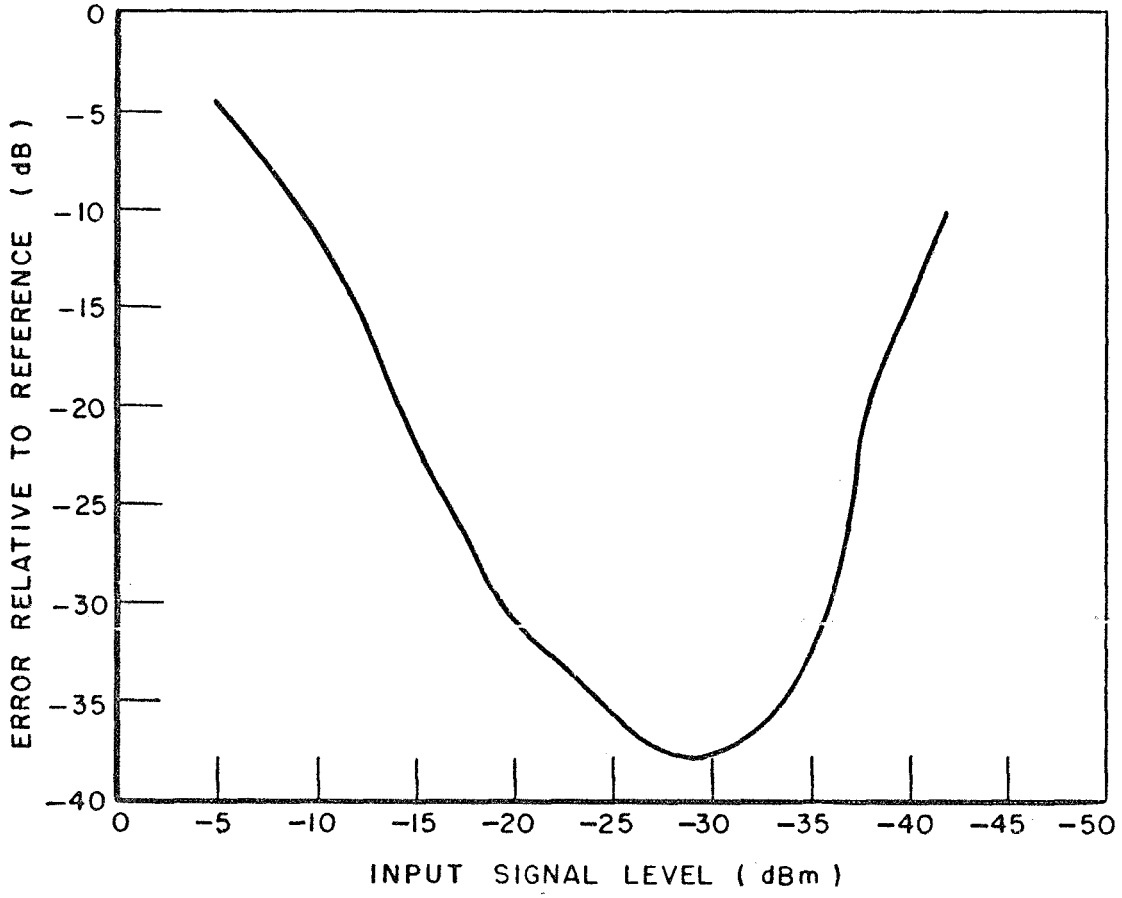

Fig. 9. Error level vs signal level.

C. Interference Rejection

Next we discuss a number of experiments dealing with the interference rejection capability of the array. As discussed above, any signal not represented in the reference signal T(t) contributes directly to the error signal, and the feedback system adjusts the weights to minimize it.

The first experiment involved a simulated test of interference rejection by the array. Two CW signals were injected directly into the processing units (i.e., no actual antenna elements were used). The signals were separated 10 kHz in frequency. First, one of them was injected with equal phase on each processing unit, corresponding to a desired signal arriving from broadside. This signal was also used for the reference signal T(t). The weighting coefficients were allowed to adapt, and the final values were noted and used to compute the pattern labelled "before adaptation" in Fig. 10. Next, a second signal (an interfering signal) was also injected, with an electrical phase angle between the units corresponding to a signal incident from 40° off broadside with half-wavelength spacing between elements. After this signal was turned on, the weighting coefficients changed to new values. These values were then used to compute the second pattern, labelled "after adaptation" in Fig. 10. It may be seen how the adaptive feedback causes the antenna to form a null on the interfering signal.

The second experiment performed was a measurement of the improvement in the ratio of desired signal power to interfering signal power at the output of the array due to the adaptive feature. First, a desired signal arriving from broadside was injected in the array. After the weighting coefficients reached their final values, they were frozen and the interfering signal was turned on. The ratio of desired signal power to interfering signal power at the output of the array was measured. The array coefficients were then allowed to readapt, and after they reached their new final values, the ratio of the powers of the desired and interfering signals was again measured. The improvement in this ratio, which we may call the adaptivity,

$$\text{Adaptivity} = \frac{\frac{D}{I} \text{ after adaptation}}{\frac{D}{I} \text{ before adaptation}}$$

where

D = desired signal power

I = interfering signal power

is plotted in Fig. 11. The figure shows the adaptivity in dB versus the electrical phase angle difference between elements for the interfering signal. The desired signal arrived from broadside (in phase in both elements) for the entire curve. The adaptivity is shown for five different interfering signal power levels at the input to the array. For all curves (except the 0 dB one) the interfering signal power is higher than that of the desired signal. The type of feedback used (see Eq. (27)) has the property that it tends to hold the error signal at a relatively constant level, regardless of the power level of the

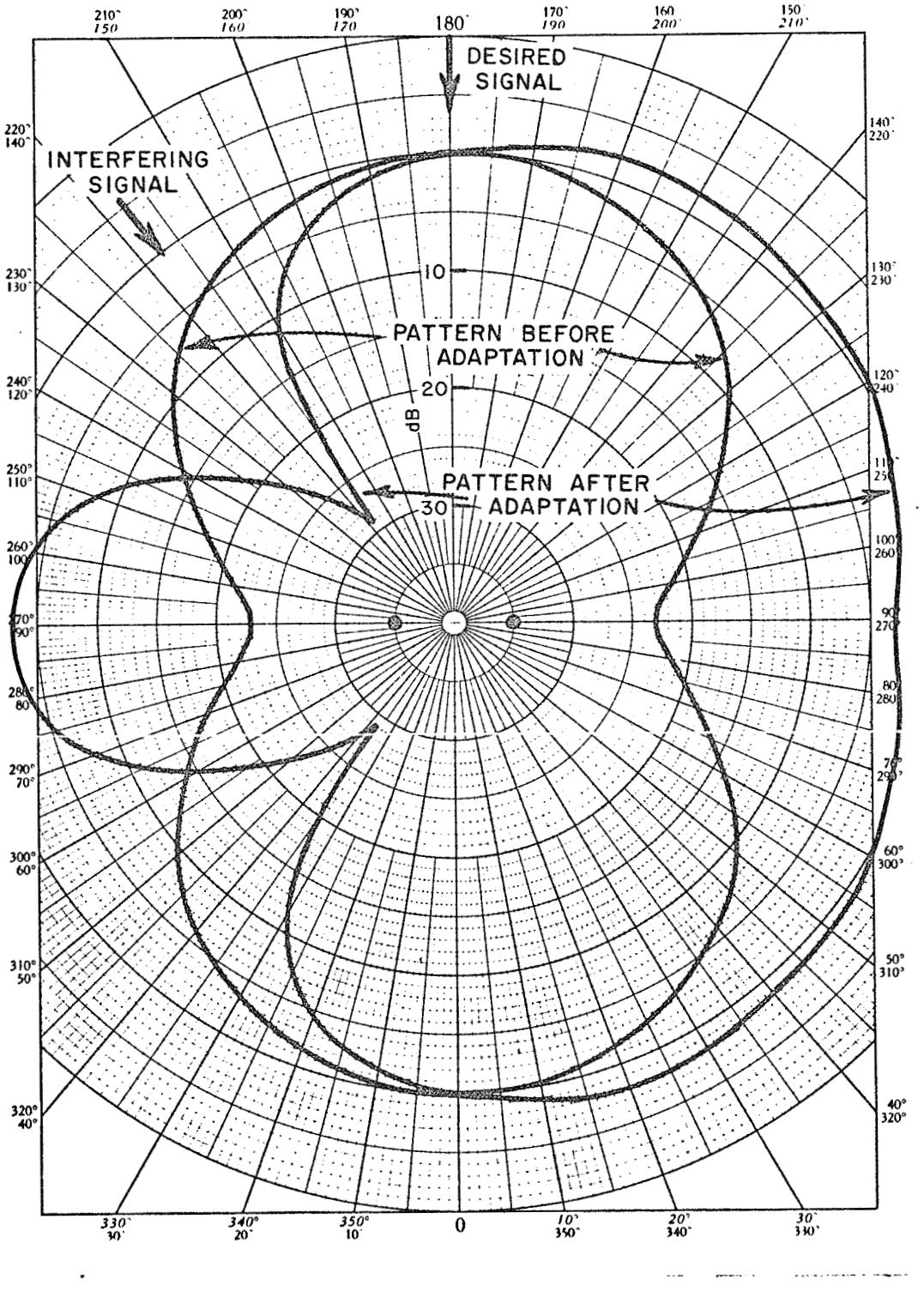

Fig. 10. Patterns before and after Adaptation.

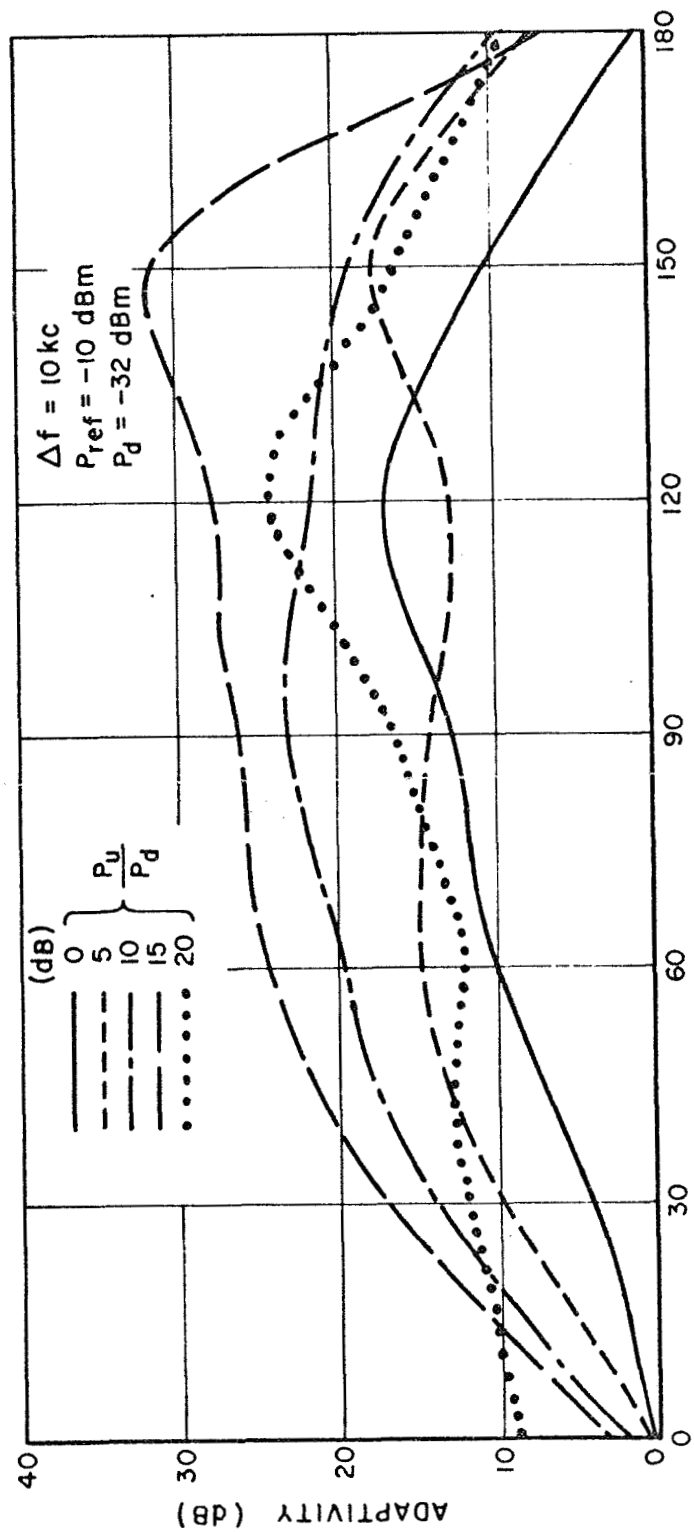

Fig. 11. Adaptive Array Improvement Over 2 Element Phased Array.

interfering signal.* This property projects into the adaptivity curves in Fig. 11. When the interfering signal power is increased 5 dB, the error signal remains constant, so the adaptivity increases 5 dB.

For the case where the interfering signal power is 20 dB higher than the desired signal power, the processing units have been driven beyond their linear limits and the units no longer operate properly.

It it noted that the adaptivity drops to zero at both ends of the curve, where the electrical phase angle between the interfering signal in the two elements approaches 0^{o} or 180^{o}. Near 180^{o}, this result is simply due to the fact that the array pattern, when maximized for broadside, has a null in the endfire direction anyway. That is, a desired signal incident from broadside results, in the absence of interference, in a pattern with a null in the endfire direction. When the interference is then turned on, it is already in a null, so the adaptive feedback makes very little change. This results in a measured adaptivity of nearly zero, but it represents no real limitation to array performance.

The drop in adaptivity near 0^{o}, on the other hand, represents the actual limitation in the system. This end of the curve defines how close the interfering signal can come to the desired signal in space and still be nulled out.

These curves show that 10 dB improvement of signal-to-interference ratio is quite easily achieved in such an array for most interference angles, and 30 dB is even possible under some conditions. Furthermore, this improvement is based on only two elements, and one may hope to do better with more elements.

Next we consider some interference rejection experiments in which actual antenna elements were used, and antenna patterns were taken on a pattern recorder. The antennas used were a pair of $\lambda/4$ monopoles** spaced $\lambda/2$ apart on a rectangular ground plane. The patterns were recorded at 2.1 gHz. Each element was connected directly to a mixer, where the frequency was converted to 65 mHz and put into the two processing units. A common local oscillator fed both mixers.

In Fig. 12, a single desired signal illuminates the antenna from the direction shown. The weighting coefficients were allowed to adapt, and were then frozen. With the weights frozen, the pattern was run, and Fig. 12 shows the result.

---

*The feedback loop for each element is a Type I (coupled) loop with loop gain proportional to the signal intensity squared. See Section D below.

**λ is the wavelength.

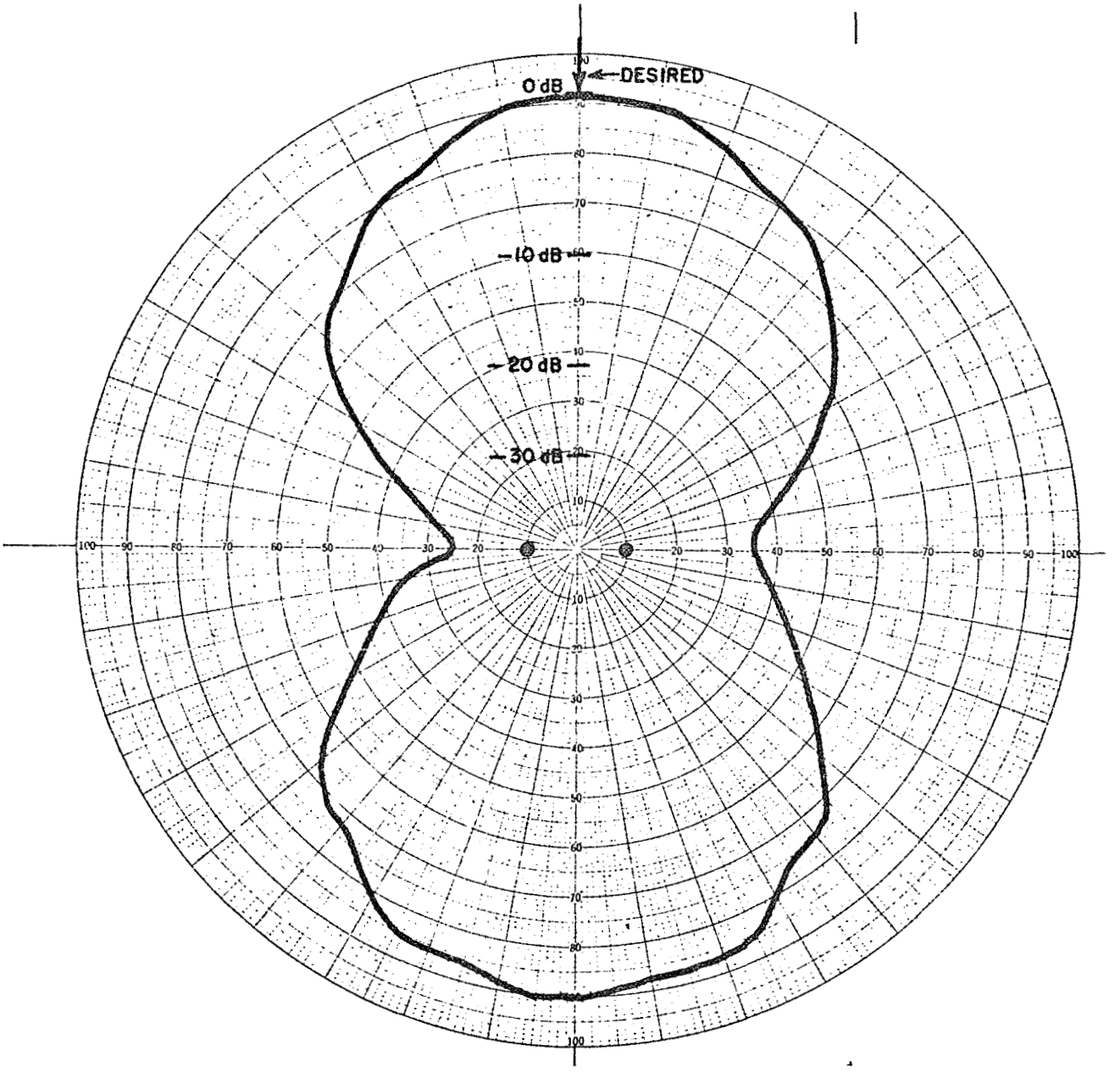

Fig. 12. Adaptive Antenna Pattern; Desired Signal Only.

In Fig. 13, the experiment was the same as for Fig. 12, except that now the array weighting coefficients were allowed to adapt as the pattern recorder turned. In this case the weighting coefficients were varying as the recorder turned, and the pattern beam tracked the signal, resulting in an "omnidirectional" pattern.

In Figs. 14, 15, and 16, both a desired signal and an interfering signal illuminated the antenna. The weights were allowed to adapt and were then frozen. The patterns shown in the figures were run with the weights fixed. These patterns show three different sets of incidence angles for the desired and interfering signals. It may be seen how the adaptive feedback forced a null in the direction of the interfering signal.

Finally, Fig. 17 shows the depth of the null on the interfering signal as a function of its angle of arrival, when the desired signal remains at broadside. (This is not an instantaneous pattern, but a plot of null depth.)

D. Speed of Response

To study the transient behavior of the weighting coefficients, one may examine the differential equations which they satisfy. Since

$$\frac{dw_i}{dt} = k_s x_i(t)\, \varepsilon(t), \tag{28}$$

and

$$\varepsilon(t) = T(t) - \sum_{j=1}^{N} w_j x_j(t), \tag{29}$$

we find

$$\frac{dw_i}{dt} = k_s x_i(t) \left[T(t) - \sum_{j=1}^{N} w_j x_j(t)\right], \tag{30}$$

or

$$\frac{dw_i}{dt} + k_s x_i(t) \sum_{j=1}^{N} x_j(t) w_j = k_s x_i(t)\, T(t). \tag{31}$$

Written in matrix form, this is

$$\frac{dw}{dt} + k_s\, X\, w = k_s\, Tx, \tag{32}$$

where w is defined in Eq. (6),

$$(33)^* \qquad X = \begin{pmatrix} x_1(t)\,x_1(t) & x_1(t)\,x_2(t) & \cdots & x_1(t)\,x_N(t) \\ x_2(t)\,x_1(t) & \cdots & & \vdots \\ \vdots & & & \vdots \\ x_N(t)\,x_1(t) & \cdots & & x_N(t)\,x_N(t) \end{pmatrix}$$

and

$$(34)^* \qquad x = \begin{pmatrix} x_1(t) \\ x_2(t) \\ \vdots \\ x_N(t) \end{pmatrix} .$$

Unfortunately, Eq. (32) is a system of differential equations for which no method of constructing a general solution is known. For the special case where there is only one weight, say w_1, Eq. (32) becomes

$$(35) \qquad \frac{dw_1}{dt} + k_s x_1^2(t) w_1 = k_s\, T(t)\, x_1(t).$$

A general solution for this equation is easily obtained by use of an integrating factor, with the result

$$(36) \qquad w(t) = e^{-\int k_s x_1^2(t)dt} \left\{ \int k_s x_1(t) T(t) e^{\int k_s x_1^2(t)dt}\, dt + C \right\}$$

where C is a constant of integration. But when more than one weight is involved, no general solution for the system (32) can be constructed. There are certain special cases, of course, where the system can be solved. For example, if the matrix X is constant, a solution is easily found. Or, if the signals happen to be such that the product of the matrices X and dX/dt commutes, then a matrix integrating factor can be used to construct a solution analogous to Eq. (36). However, these cases do not appear to correspond to a meaningful set of signals in the adaptive array problem.

---

*Note that $\phi(x,x) = \overline{X}$, $\phi(x,T) = \overline{T(t)x}$.

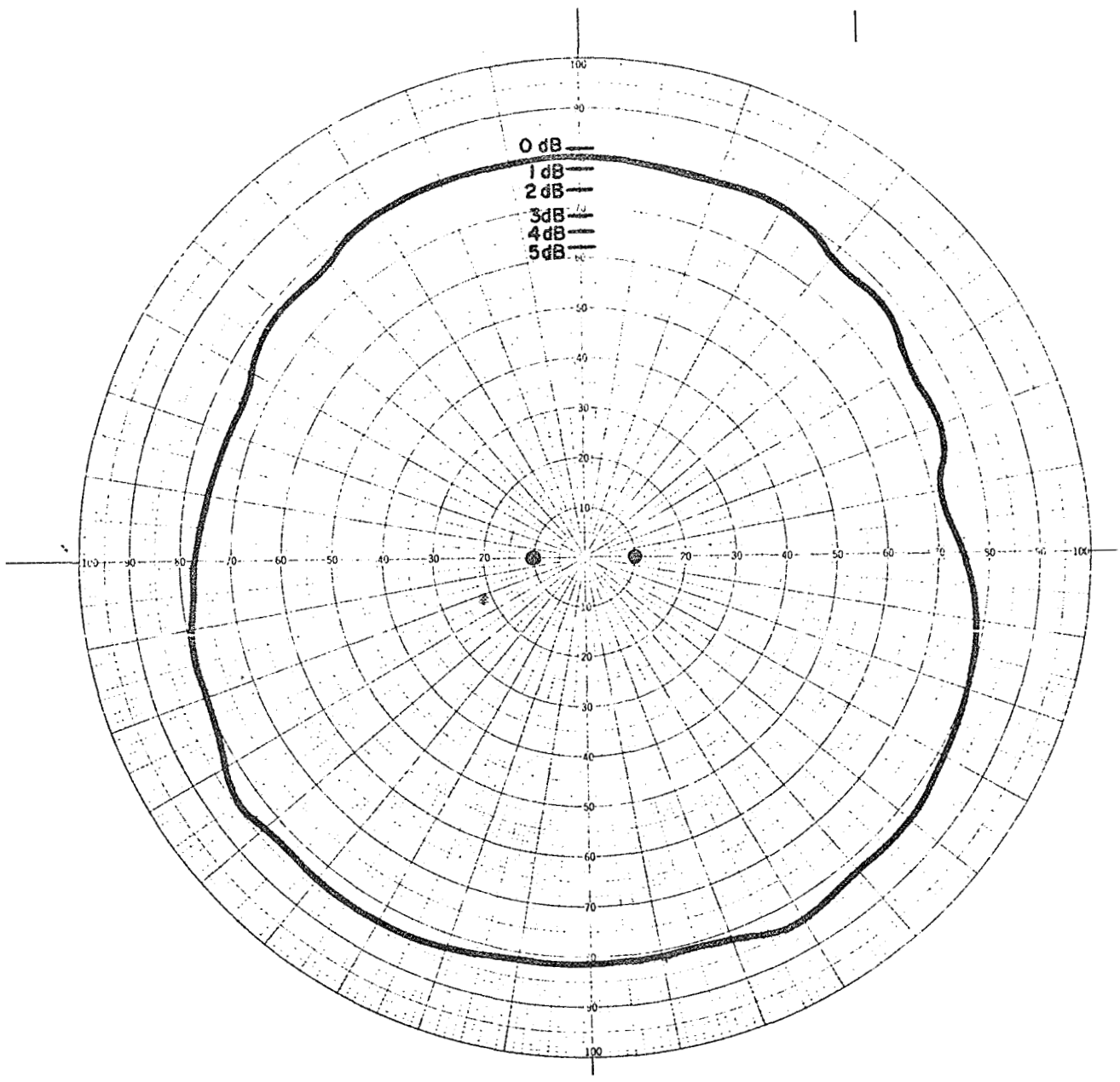

Fig. 13. Adaptive Antenna Pattern; Desired Signal Tracked.

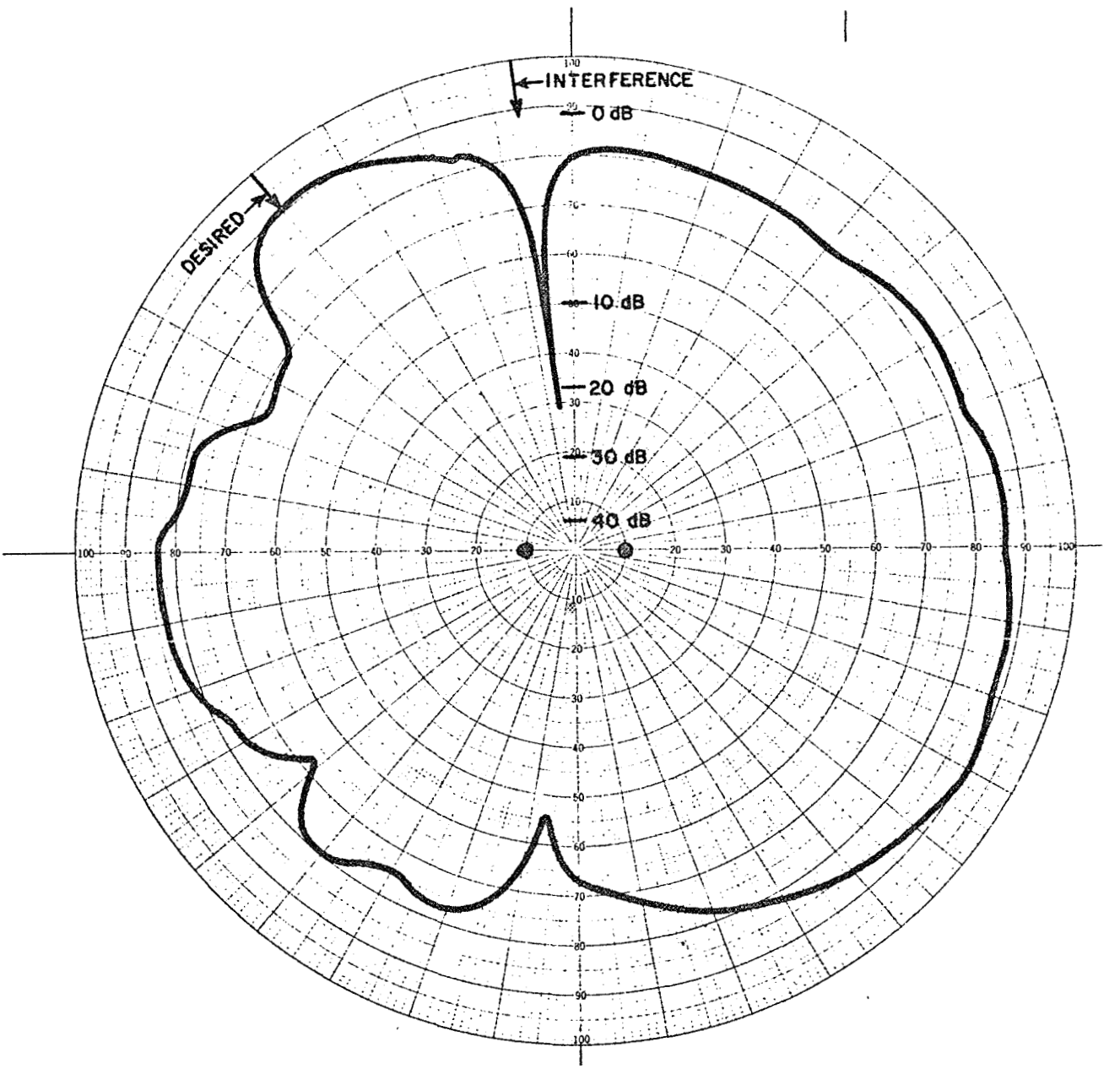

Fig. 14. Adaptive Antenna Pattern; Desired Signal Plus Interference.

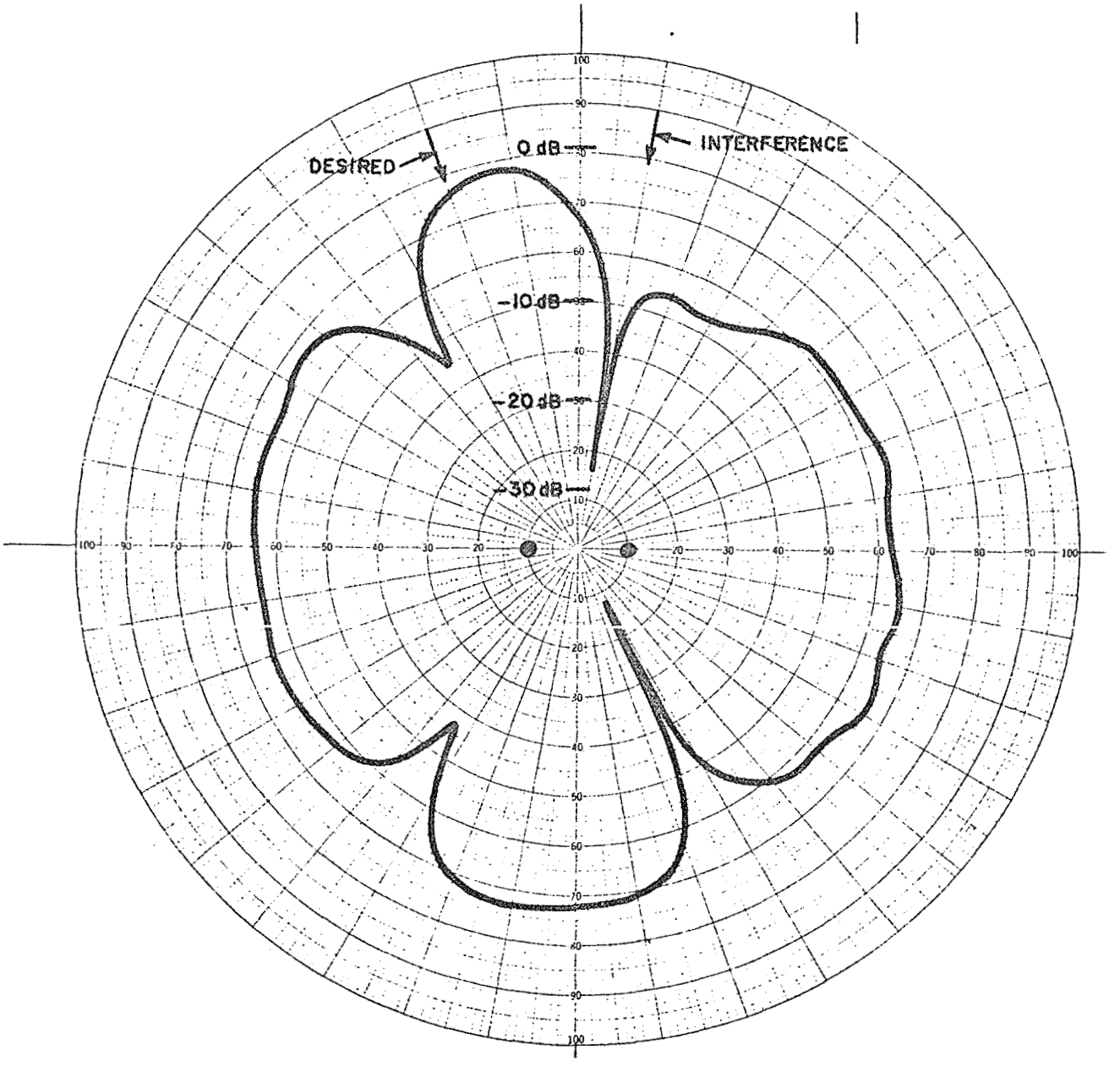

Fig. 15. Adaptive Antenna Pattern; Desired Signal Plus Interference.

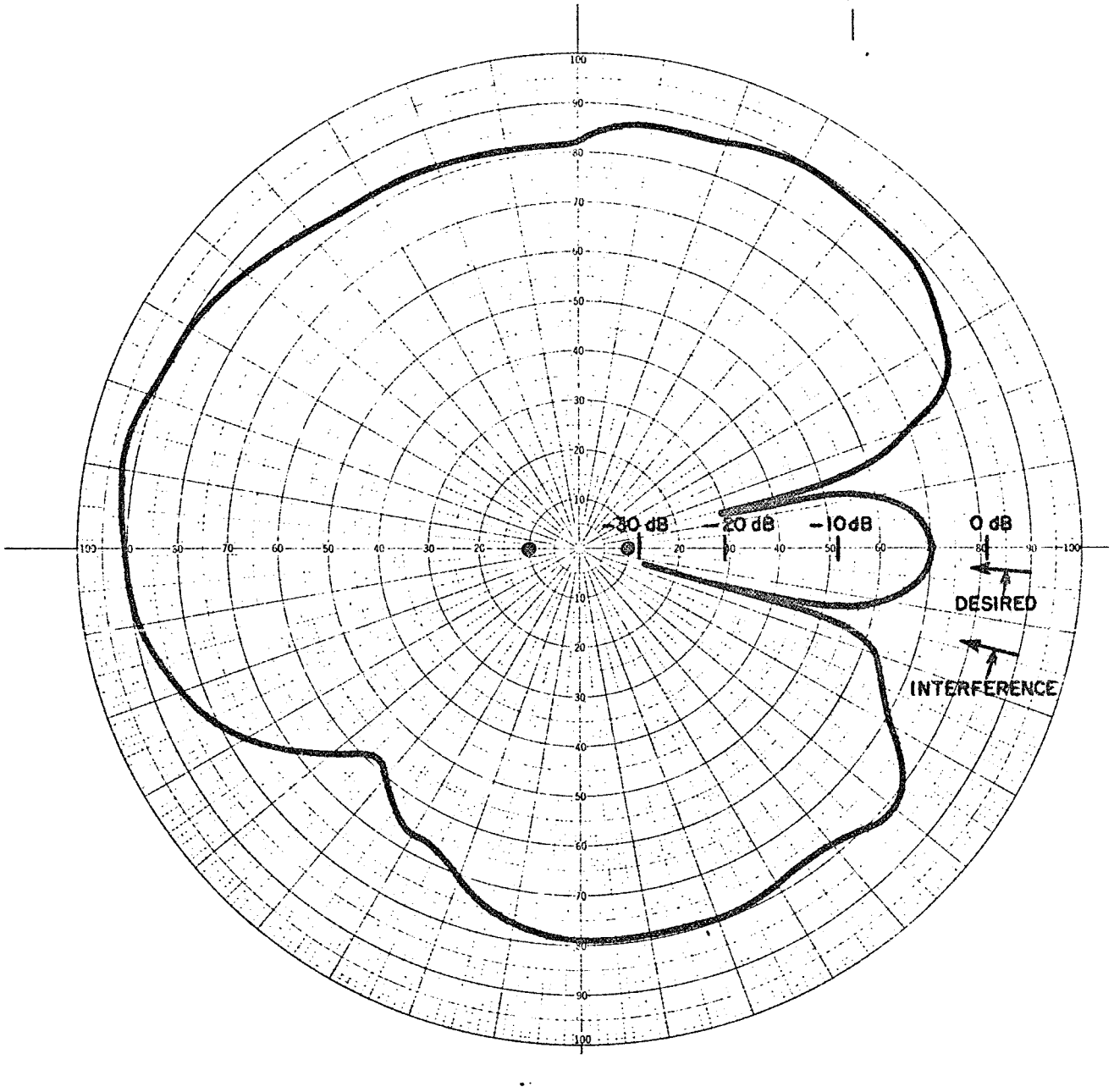

Fig. 16. Adaptive Antenna Pattern; Desired Signal Plus Interference.

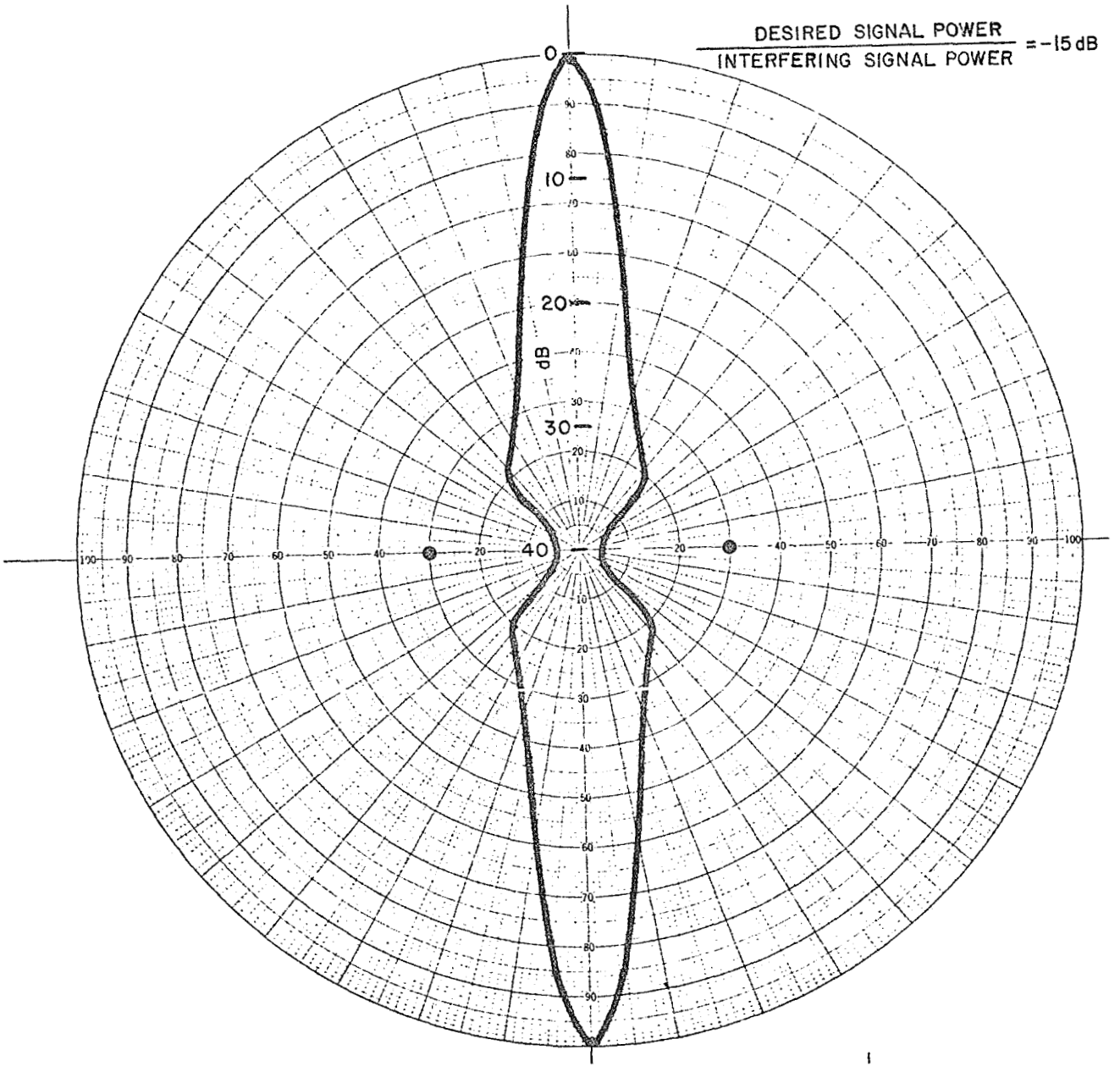

Fig. 17. Depth of Interference Null.

Other approaches to solving the system (32) are of course possible. The equations can be solved on an analog computer or a digital computer. Various techniques for obtaining approximate analytical solutions, such as series solutions or perturbation techniques, seem promising. These ideas are presently under study, and will be discussed in a future report.

Certain general conclusions are possible, however. When this system is viewed as a problem in feedback control, it is clear that the response time of the system depends on the amplitudes of both the desired and interfering signals, because of the $x_i(t)\ x_j(t)$ terms in the differential equations. Stated another way, the feedback loop has a gain constant proportional to the square of the signals $x_i(t)$. Hence the larger the signals $x_i(t)$, the tighter the loops. This is the reason that the error signal amplitude is approximately independent of the input signal level, as we previously remarked. In a linear feedback loop, a larger input signal would imply a larger steady state error. But for this loop, a larger input results in a tighter loop, with the result that the error stays constant.

Figure 18 shows a measured transient response of one of the weighting coefficients in the array. This curve is a typical result, and has a time constant of approximately 20 or 30 milliseconds.

E. Experiments with Modulated Signals

Next we consider some experiments where the signals in the array contain modulation but the reference signal is unmodulated. For a desired signal having amplitude modulation of the form

$$S(t) = a(t) \cos \omega_0 t \tag{37}$$

$$= A_0 [1 + 2k_m \cos \omega_m t] \cos \omega_0 t,$$

and a reference signal of the form

$$T(t) = A_r \cos \omega_0 t, \tag{38}$$

the mean-square error $\overline{\varepsilon^2(t)}$ is found to be

$$\overline{\varepsilon^2(t)} = \frac{1}{2} (A_r - A_0)^2 + (A_0 k_m)^2 \tag{39}$$

The value of A_0 giving least $\overline{\varepsilon^2(t)}$ may be found by setting

$$\frac{\partial \varepsilon^2(t)}{\partial A_0} = 0, \tag{40}$$

which yields

$$(41) \qquad A_o = \frac{A_r}{1 + 2k_m^2}$$

Hence the minimum mean-square error criterion does not force the carrier component of the AM signal to be equal to the reference signal carrier. Instead the carrier of the AM signal is suppressed relative to the reference carrier, by an amount dependent on the modulation factor k_m.

Figure 19 compares this calculated suppression with the results measured on the processing units, for two different signal levels. For $k_m = 0$, A_o should be equal to A_r and no suppression should occur. For $k_m = \frac{1}{2}$ (100% modulation) $A_o = 2/3\ A_r$ and the carrier of the signal should be about 3.5 dB lower than the reference signal. The experimental results shown in Fig. 19 agree reasonably well with this.

Next, we consider the interference rejection properties of the array with modulated signals. Figures 20-22 show photographs taken of a spectrum analyser connected to the output of the array. In Fig. 20, the desired signal consists of a carrier component and two sidebands separated 50 kHz from the carrier. The carrier of the desired signal was used for the reference signal (that is, the reference signal did not contain the modulation components). A CW interfering signal was added 10 KHz below the carrier of the desired signal. The top photo shows the output spectrum before the weighting coefficients are allowed to adapt, and the bottom curve shows it after adaptation. It may be seen how the interference is removed from the output by the adaptive feedback. In Figs. 20-22, the spectrum analyser has a linear voltage scale. In Fig. 20, the interfering signal has approximately 4 times the voltage of the desired signal carrier, or 16 times the power.

Figure 21 shows a case in which both the desired signal and the interfering signal are modulated. The desired signal has sidebands 50 kHz from the carrier, and the carrier alone is also used for the reference signal, as before. The interference has a carrier approximately 8 kHz below the carrier of the desired signal, and modulation sidebands 20 kHz each side of the carrier. The pictures again show the spectra before and after adaptation.

Finally, Fig. 22 shows a case involving noise modulation on the interfering signal. Photo (a) shows the spectrum of the desired signal alone. (The carrier of the desired signal was used for the reference signal.) Photo (b) shows the output from the array when the interference is added, but before adaptation. Photo (c) shows the output again after adaptation.

The manner in which the adaptive feedback cleans out the interference in these tests is very impressive, and it is clear that these antennas have considerable potential for applications where interference rejection is needed.

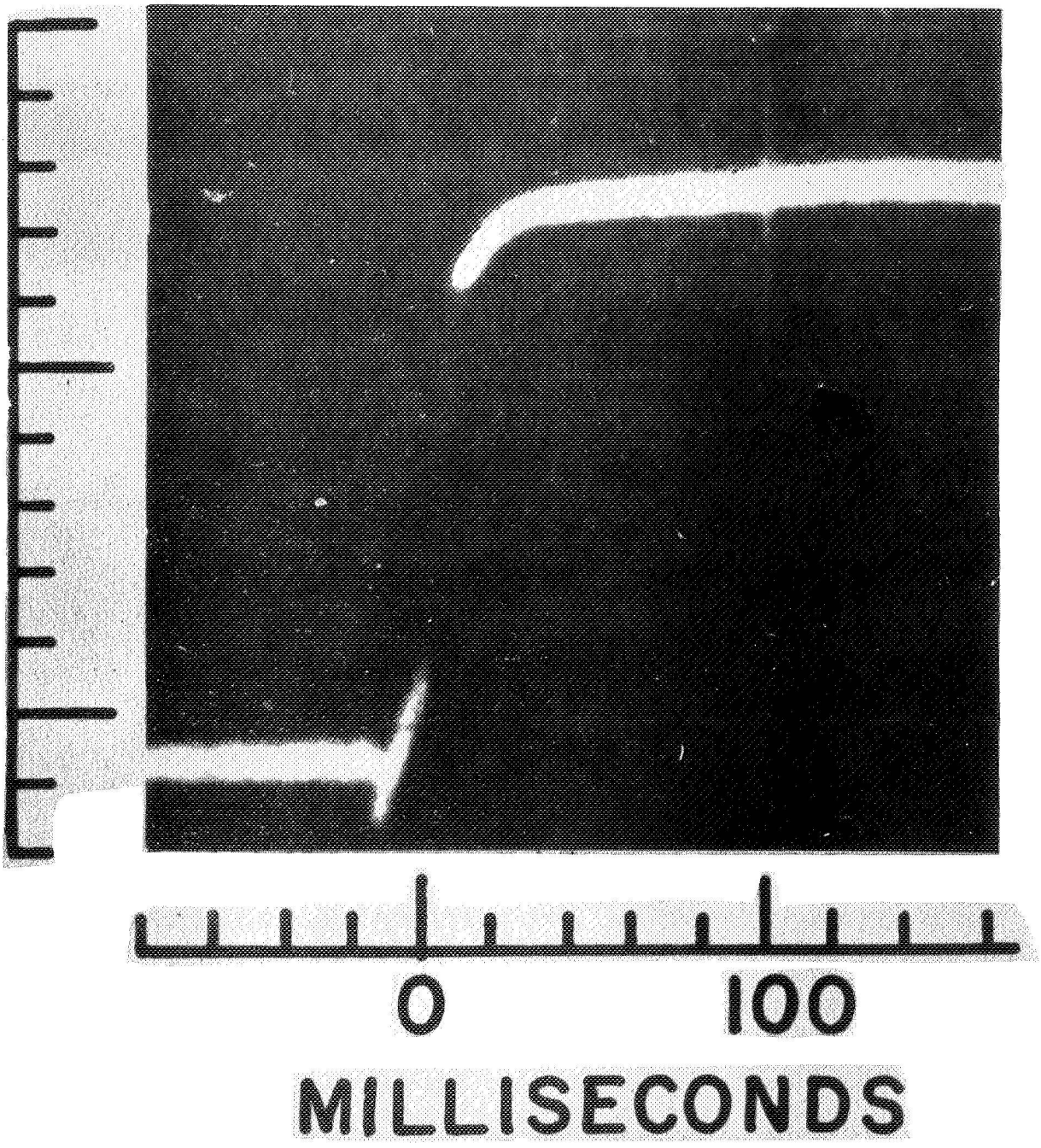

Fig. 18. Time response of weighting coefficient.

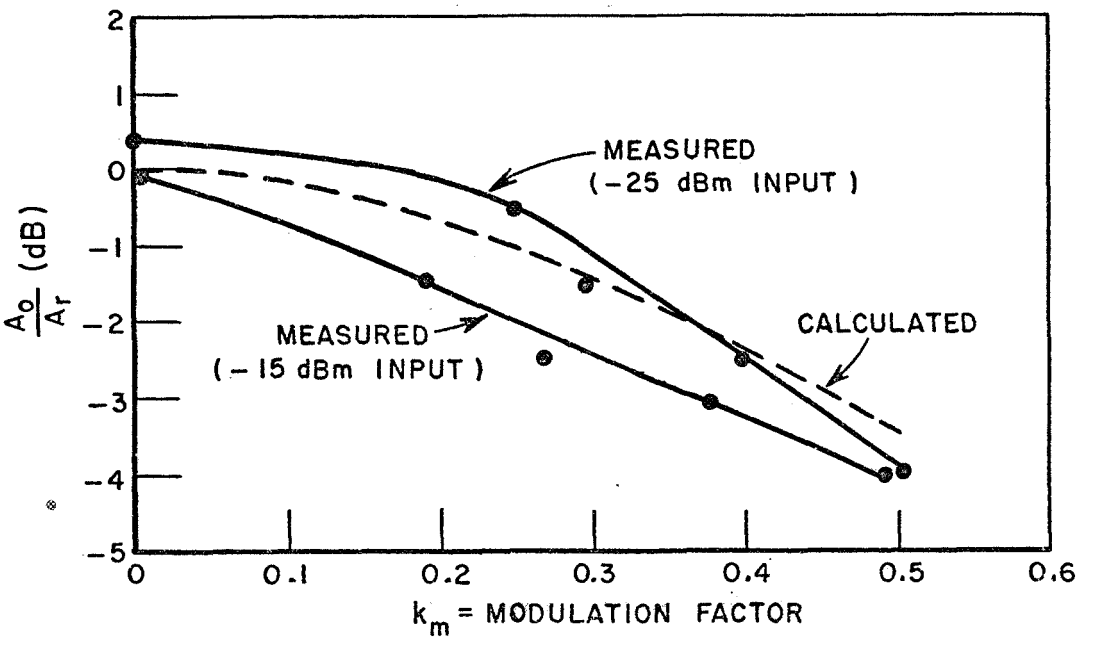

Fig. 19. Effect of modulation on desired signal.

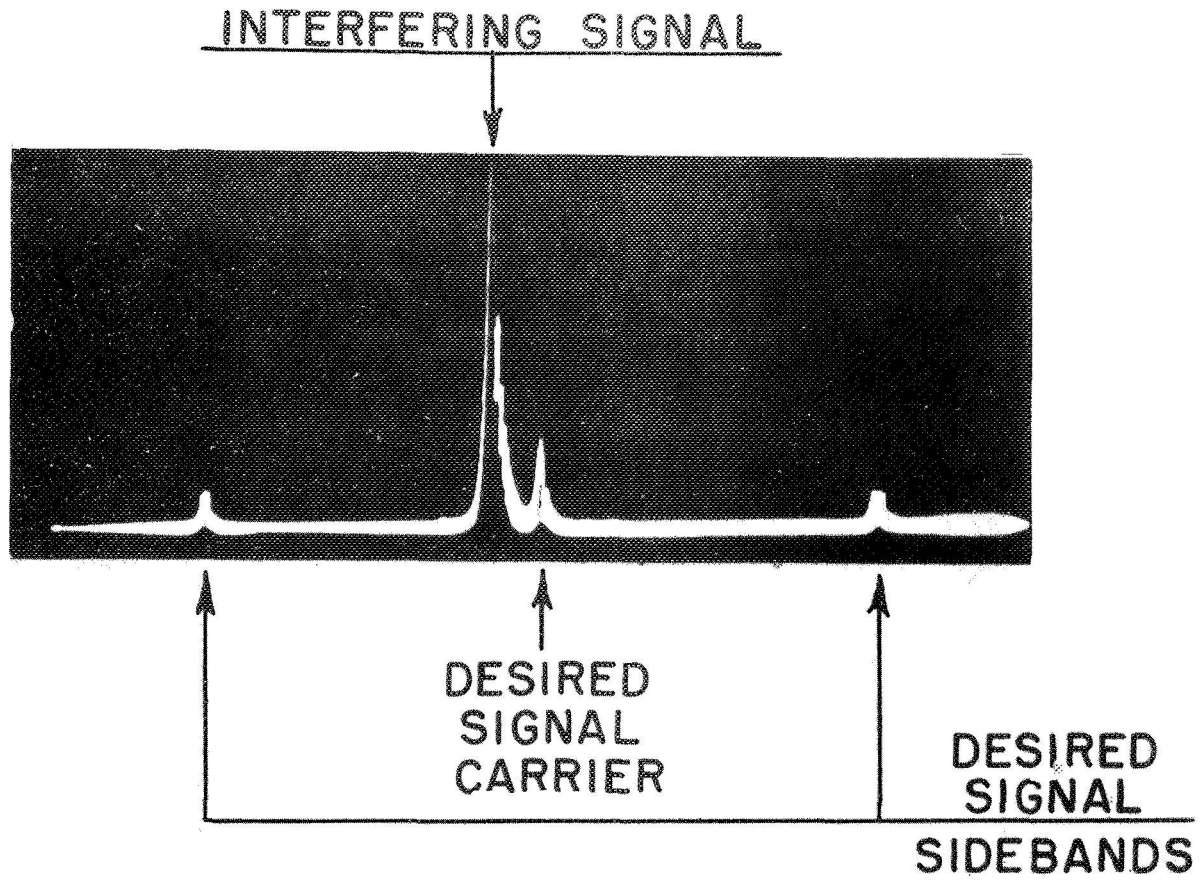

(a) BEFORE ADAPTATION

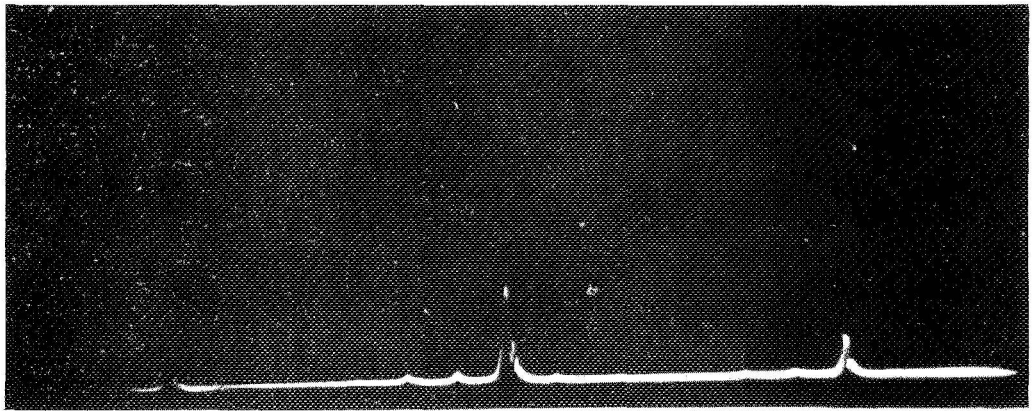

(b) AFTER ADAPTATION

Fig. 20. Adaptive rejection of interfering signal.

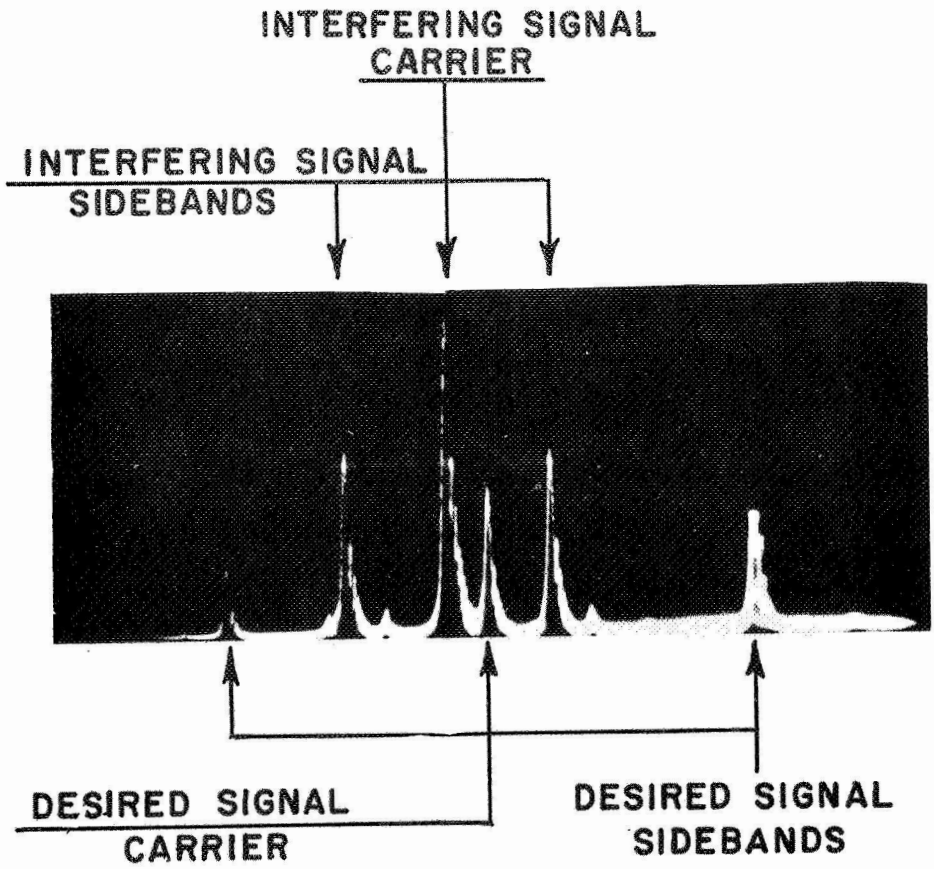

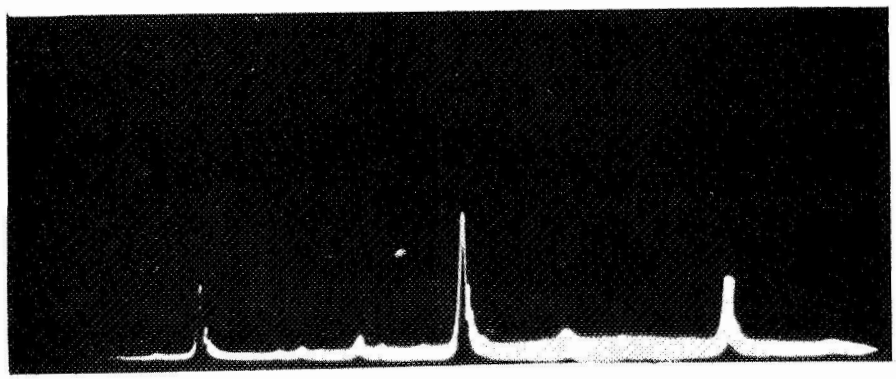

Fig. 21. Adaptive rejection of interfering signal.

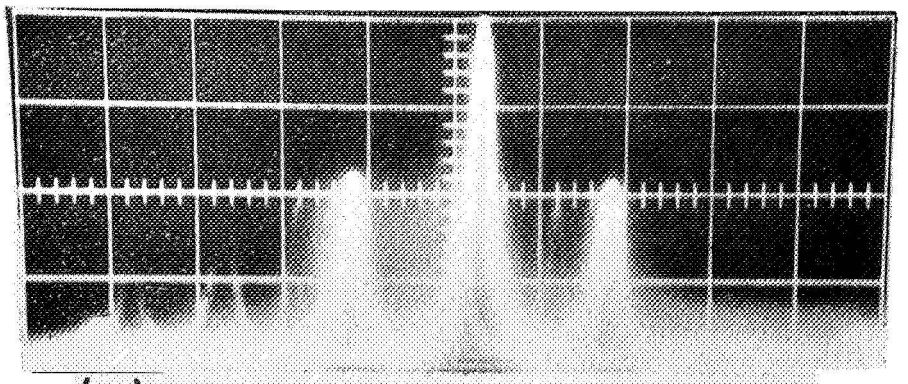

(a) SPECTRUM OF DESIRED SIGNAL

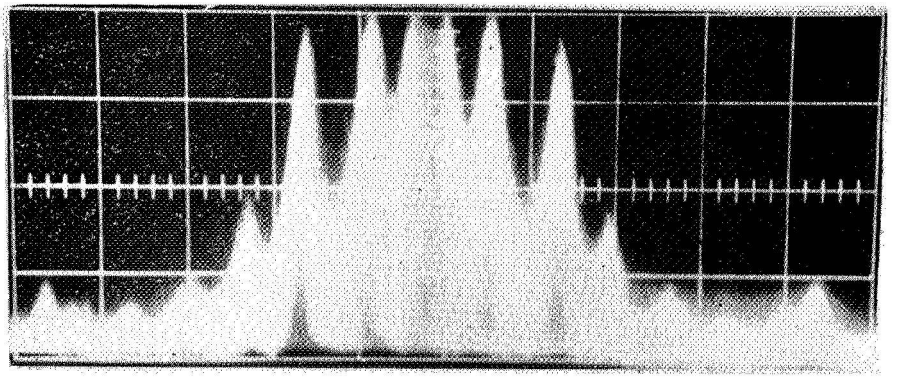

(b) ARRAY OUTPUT SPECTRUM BEFORE ADAPTATION (DESIRED) SIGNAL PLUS INTERFERING SIGNAL

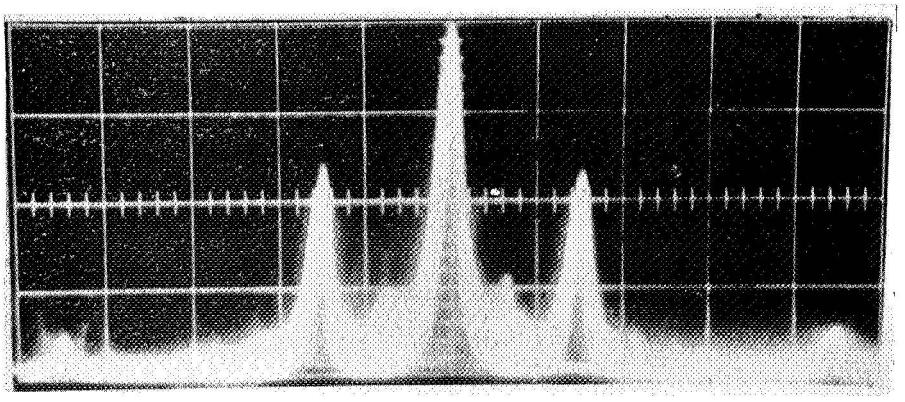

(c) ARRAY OUTPUT SPECTRUM AFTER ADAPTATION (DESIRED) SIGNAL PLUS INTERFERING SIGNAL

Fig. 22. Adaptive rejection of interfering signal.

V. CONCLUSIONS

An experimental two-element array has been described. The array operation is based on a feedback algorithm determined by a steepest-descent minimization of error. The array is found to be capable of automatically tracking a desired signal, and automatically rejecting an interfering signal.

A number of experiments were performed on the two-element array, including

(1) measurements of the ability of the processing units to track phase and amplitude of the desired signal (Figs. 8 and 9),

(2) measurements of the "adaptivity" of the array (Figs. 10 and 11),

(3) measurements of antenna patterns obtained with interference present (Figs. 12-17),

(4) measurements of the transient response of the system (Fig. 18), and

(5) measurements of the interference rejection capabilities with modulated signals (Figs. 20-22).

The tests described show that these antennas have considerable potential for applications where interference rejection is needed. The signal processing equipment is straightforward and can be constructed with readily available components.

APPENDIX

This section presents the circuit diagram for a signal processor and briefly describes the components used. The schematic is given in Fig. A1. Except for the $\lambda/4$ delay line both the upper and lower halves are symmetrical.

A double-balanced mixer using four matched hot carrier diodes was used to perform the multiplication operation. The excellent balance of the mixer eliminated the need for null balance adjustment and minimized the interaction between the incoming and error signals.

A high gain discrete component operational amplifier with RC feedback was used for the integrator. A unity gain integrated circuit amplifier provided the required sign inversion.

Dual gate field effect transistors were used both to provide gain and to vary the weighting coefficient for each of the four channels of the signal processor. A single gate FET could have been used to provide power gain but the dual gate version is reported to have superior cross-modulation performance and greater dynamic range.

The nearly infinite dc gate impedance of this device provides an excellent means for "freezing" the weighting coefficients. By simply disconnecting the control voltage from the gate, with a switch, the amplifier gain remains constant and one can then run an antenna pattern. The amplifier gain remains constant for several hours with no measurable change from the previous closed loop value.

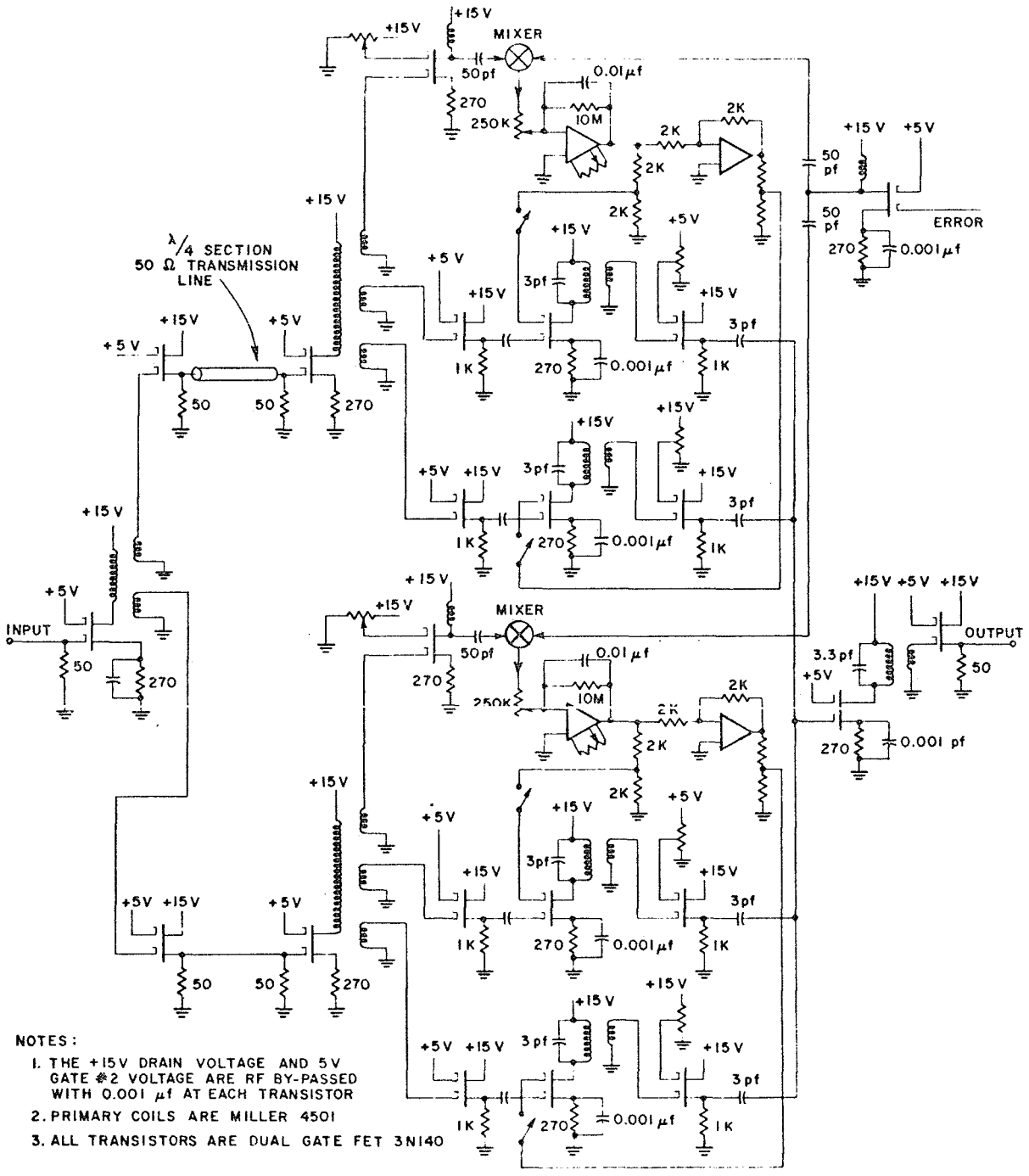

Fig. A1. Circuit diagram of processing unit.

REFERENCES

1. Svoboda, D.E., "A Phase-Locked Receiving Array for High-Frequency Communications Use," IEEE Transactions on Antennas and Propagation, AP-12, 2 (March 1964), 207-215.

2. Brennan, D.G., "Linear Diversity Combining Techniques," Proc. IEEE, 47, 6 (June 1959), 1075-1102.

3. Svoboda, op cit., see Fig. 8.

4. Shor, S.W.W., "Adaptive Technique to Discriminate Against Coherent Noise in a Narrow-band System," J. Acoust. Soc. Am., 39, (January 1966), 74-78.

5. Widrow, B., P.E. Mantey, L.J. Griffiths, and B.B. Goode, "Adaptive Antenna Systems," Proc. IEEE, 55, 12 (December 1967), 2143-2159.